AD_____

Award Number: DAMD17-99-1-9073

TITLE: Research Training Program in Breast Cancer

PRINCIPAL INVESTIGATOR: Daniel Medina, Ph.D.

CONTRACTING ORGANIZATION: Baylor College of Medicine
Houston, Texas 77030

REPORT DATE: July 2000

TYPE OF REPORT: Annual Summary

PREPARED FOR: U.S. Army Medical Research and Materiel Command
Fort Detrick, Maryland 21702-5012

DISTRIBUTION STATEMENT: Approved for Public Release;
Distribution Unlimited

The views, opinions and/or findings contained in this report are those of the author(s) and should not be construed as an official Department of the Army position, policy or decision unless so designated by other documentation.

REPORT DOCUMENTATION PAGE

Form Approved
OMB No. 074-0188

1. AGENCY USE ONLY (Leave blank)	2. REPORT DATE	3. REPORT TYPE AND DATES COVERED
	July 2000	Annual Summary (1 Jul 99 - 30 Jun 00)

4. TITLE AND SUBTITLE
Research Training Program in Breast Cancer

5. FUNDING NUMBERS
DAMD17-99-1-9073

6. AUTHOR(S)
Daniel Medina, Ph.D.

7. PERFORMING ORGANIZATION NAME(S) AND ADDRESS(ES)
Baylor College of Medicine
Houston, Texas 77030

E-MAIL:
dmedina@bcm.tmc.edu

8. PERFORMING ORGANIZATION REPORT NUMBER

9. SPONSORING / MONITORING AGENCY NAME(S) AND ADDRESS(ES)
U.S. Army Medical Research and Materiel Command
Fort Detrick, Maryland 21702-5012

10. SPONSORING / MONITORING AGENCY REPORT NUMBER

11. SUPPLEMENTARY NOTES

12a. DISTRIBUTION / AVAILABILITY STATEMENT
Approved for public release; distribution unlimited

12b. DISTRIBUTION CODE

13. ABSTRACT *(Maximum 200 Words)*

The goal of this research training program is to produce highly qualified scientists for careers as independent investigators in the field of breast cancer. During the last 25 years, there has been a fundamental revolution in the understanding of molecular and cell biological concepts related to cell growth, function and tumorigenesis. To utilize what has been learned and to continue future progress in the area of breast cancer requires the continued availability of well-trained, innovative and committed scientists. This program represents an interdepartmental training program involving fifteen investigators from seven departments. Trainees are predoctoral and postdoctoral fellows with backgrounds in biochemistry, cell and molecular biology, molecular genetics and molecular virology. The training program provided trainees with additional foundation in carcinogenesis and breast cancer. In addition to the core curriculum taken by the predoctoral fellows in their respective academic departments, program enhancement is provided through trainees' participation in a graduate course on "Molecular Carcinogenesis" (predoctoral fellows), a Breast Cancer Seminar Series (all trainees) and participation at national meetings and local seminars. Four predoctoral and two postdoctoral trainees are enrolled in the training program.

14. SUBJECT TERMS	15. NUMBER OF PAGES
Breast Cancer	37
	16. PRICE CODE

17. SECURITY CLASSIFICATION OF REPORT	18. SECURITY CLASSIFICATION OF THIS PAGE	19. SECURITY CLASSIFICATION OF ABSTRACT	20. LIMITATION OF ABSTRACT
Unclassified	Unclassified	Unclassified	Unlimited

NSN 7540-01-280-5500

Standard Form 298 (Rev. 2-89)
Prescribed by ANSI Std. Z39-18
298-102

FOREWORD

Opinions, interpretations, conclusions and recommendations are those of the author and are not necessarily endorsed by the U.S. Army.

___ Where copyrighted material is quoted, permission has been obtained to use such material.

___ Where material from documents designated for limited distribution is quoted, permission has been obtained to use the material.

___ Citations of commercial organizations and trade names in this report do not constitute an official Department of Army endorsement or approval of the products or services of these organizations.

X In conducting research using animals, the investigator(s) adhered to the "Guide for the Care and Use of Laboratory Animals," prepared by the Committee on Care and use of Laboratory Animals of the Institute of Laboratory Resources, national Research Council (NIH Publication No. 86-23, Revised 1985).

N/A For the protection of human subjects, the investigator(s) adhered to policies of applicable Federal Law 45 CFR 46.

N/A In conducting research utilizing recombinant DNA technology, the investigator(s) adhered to current guidelines promulgated by the National Institutes of Health.

N/A In the conduct of research utilizing recombinant DNA, the investigator(s) adhered to the NIH Guidelines for Research Involving Recombinant DNA Molecules.

N/A In the conduct of research involving hazardous organisms, the investigator(s) adhered to the CDC-NIH Guide for Biosafety in Microbiological and Biomedical Laboratories.

Daniel Medina 7-20-00

PI - Signature Date

Table of Contents

5. INTRODUCTION

Breast cancer is a complex disease whose ultimate understanding will require the integration of facts resulting from a multidisciplinary approach. Continued basic science research will provide a fuller understanding of the basic mechanisms of breast cancer that is necessary to conquer the disease in humans. In order to have the scientific human armamentarium to further this understanding, this training grant focuses on producing qualified scientists for careers as independent investigators in the area of breast cancer. The rationale for a targeted training grant in breast cancer is based on the belief that the elucidation of how oncogenes, tumor suppressor genes, hormones and growth factors act at the molecular level and as developmental-specific agents are critical questions directly relevant to the etiology, prevention, diagnosis, treatment and prognosis of human breast cancer. The training program has drawn together individuals who have an established research and training background in the mammary gland with individuals who have a research and training background in cell biology, molecular endocrinology, molecular biology, molecular virology, viral oncology, molecular genetics and biochemistry. The strength of the program is two-fold. First, the program gathers together members of diverse disciplines to focus on the training of predoctoral and postdoctoral students for careers in an area that, by its biological nature, is multi-disciplinary. Second, the program introduces new intellectual approaches and insights to the problem of breast cancer that will be continued by the next generation of research scientists.

The design of the training program provides for trainees to be exposed to clinical problems and recent advances as well as the multi-disciplinary approaches to answering fundamental questions related to breast cancer research. The familiarity and close proximity of the training faculty facilitates and encourages the development of a new generation of research scientists who will be able to understand the problem of breast cancer at a more complex level and from a multi-disciplinary orientation.

6. BODY OF PROPOSAL

a. Trainees

The goal of this training program is to provide an environment for training in breast cancer research. To foster this goal, candidate graduate students have to meet a minimum set of requirements. Graduate students have to be at least in their second year of graduate school and have selected a thesis problem focusing on an aspect of mammary gland growth, differentiation and/or cancer. These students are supported for two years by the training program provided they maintain satisfactory progress in their research program and they participate in the weekly "Breast" seminar and attend the course "Molecular Carcinogenesis". The two postdoctoral fellows are supported by the training program for two to three years provided they maintain satisfactory progress in their research project and actively participate in the weekly "Breast" seminar. The six fellows from the grant year 1999-2000, their departmental affiliation, mentor, research problem and an Abstract of their research is provided below.

b. Research Projects

1) Andrew Dennis, Department of Molecular and Cellular Biology; Mentor, Bert W. O'Malley, M.D., Professor and Chairman; "Characterization of human Uba3: a novel type of nuclear hormone receptor coactivator."

ABSTRACT

The estrogen and progesterone steroids are important factors that influence cell growth and mammary gland development by binding to, and activating their cognate receptors, the estrogen and progesterone receptor (ER and PR), respectively. Coactivator proteins enhance the transcriptional activation of ligand-activated receptors several fold by acting as molecular bridges and/or chromatin remodeling enzymes. Ubiquitin-activating enzyme 3 (Uba3) is a hormone-dependent PR interacting protein identified originally by the yeast 2-hybrid system. Experiments were designed to determine whether or not Uba3 could serve as coactivator of nuclear hormone receptors, including PR. Using transient transfection assays in HeLa cells, Uba3 coactivated several steroid receptors including ERα, PR-B, glucocorticoid receptor (GR), and androgen receptor (AR), and the non-steroid receptors thyroid receptor (TRβ) and retinoic acid receptor (RARα). Significantly, coactivation of ERα and PR-B was more pronounced than the other steroid/non-steroid receptors, suggesting that Uba3 exhibits higher specificity to modulate activation of these receptors. Since coactivators can stimulate ligand-activated receptor-dependent transcription several fold, it is thought that these proteins need to be in limited cellular concentrations. Activation of both ERα and PR-B by their cognate ligands titrates or squelches away the intracellular availability of coactivators, lowering potential coactivation. Addition or exogenous Uba3 relieves this "squelching" effect between ligand-activated ERα and PR-B, indicating that Uba3 is a limiting factor. *In vitro* GST-pulldown assays were performed to study whether PR-B and Uba3 directly interact with each other. These studies are currently ongoing, however, hPR-B does bind to GSTUBA3, suggesting a direct interaction between these two proteins. Uba3 functions as an E1 (ubiquitin-activating enzyme) with another protein called APP-BP1. Mammalian expression vectors encoding the cDNA of APP-BP1 have been generated to test if APP-BP1 has an effect on the coactivation of PR. Uba3 is being

purified in an attempt to generate polyclonal rabbit antibodies to Uba3. Several serum samples are being used to establish optimal conditions. Once the use of these antibodies are optimized, Uba3 content in various breast cancer cell lines will be analyzed by Western blot at the protein level and RNase protection assay on the RNA level.

2) Yue He, Department of Molecular and Human Genetics; Mentor, Allan Bradley, Ph.D., Professor; "Tissue specific chromosome deletion: an *in vivo* genetic screen for tumor suppressor gene in mammary gland."

ABSTRACT

Breast cancer is the second most common leading cause of cancer death. A genetic contribution of breast cancer risk is indicated by the increased incidence among women with a family history of breast cancer, and by the observation of those rare families in which multiple family members are affected with breast cancer. Currently, although several genetic mutations have been identified as the cause of inherited cancer risk of many cancer-prone families, they comprise no more than 5% to 10% of breast cancer cases overall. Genes that are mutated in sporadic breast cancers are still largely unknown.

A novel genetic screen is being used to identify tumor suppressor genes mutated in sporadic breast cancer. This genetic screen utilizes the current chromosomal engineering technology in mouse, combined with the mammary gland specific expression of Cre to delete a defined region of the chromosome in mouse mammary epithelial cells *in vivo*. The Cre induced chromosomal deletion events will render cells functionally haploid for the deleted region, which should not have any functional consequence as somatic cells have higher tolerance towards larger chromosomal deficiency than embryos. A second mutation then can be introduced into the mammary epithelial cells with retrovirus infection. Mouse mammary tumor virus (MMTV) was chosen as the insertional mutagen since MMTV replicates in the mammary epithelial cells and randomly integrates into the genome. If adequate insertional events are screened, many mutations will be located in the haploid region and few of them will inactivate certain tumor suppressor genes located in this haploid region. Loss of both copies of tumor suppression gene, one by chromosomal deletion and another by insertional mutagenesis will render cells nullizygous for the gene, and accelerate clonal expansion and tumor progression process, eventually lead to the tumor formation in the mammary gland. The mutated tumor suppressor genes can then be identified by the tagged MMTV provirus. The identification of tumor suppressor genes, which are significant mutation targets in sporadic breast cancer will not only provide deeper insight into the neoplastic development in mammary gland, but will also provide useful information to clinically improve the diagnoses and treatment of breast cancer.

Three specific aims are being pursued in this project. Aim 1 is to generate several "pre-deletion" mouse lines. "Pre-deletion" chromosome carries two loxP sites in cis orientation. Mouse chromosome 11 was chosen as the target chromosome due to its homology to human chromosome 17, which is believed to contain several tumor suppressor genes based on its LOH data. The available "pre-deletion" line in the lab carries the two loxP sites between the D11Mit142 and E2DH locus, which are 34.1cM apart. Aim2 is to generate and characterize mammary gland specific Cre lines. One Cre line is driven by MMTV-LTR and in another line Cre is under the promoter of beta-casein. Currently, the Cre expression is being characterized by

crossing the Cre lines to rosa26 Reporter mice and subsequently studying the lacZ expression in the double transgenic mice. Aim3 is to examine MMTV mutagenesis in the double transgenic mouse carrying both "pre-deletion" chromosome and mammary gland specific Cre transgene.

3) Amy Tabor, Department of Molecular and Human Genetics; Mentor, Sharon Plon, M.D., Ph.D., Assistant Professor; "Targets for ATM protein kinase."

ABSTRACT

This project focuses on identifying novel targets of the ATM protein kinase. Women who are heterozygous for mutations in ATM have an increased risk of developing breast cancer. Therefore, increased knowledge of the ATM pathway will facilitate understanding mammary tumorigenesis. Two experimental methods were used to achieve this goal: the first included a two-hybrid screen using the kinase domain portion of ATM and a human cDNA library as the target. A large scale screen of this library identified three potential targets. Further analysis of these targets revealed that they did not encode authentic targets of ATM. The second approach was to look for interaction with specific candidate targets. The possibility that the human homolog of Rad21 might be an ATM target was examined. Rad21 in lower eukaryotes is required for the response to DNA damage and chromosome segregation during normal cell cycles. A variety of experiments were performed to determine the expression of Rad21 in both wild-type and ATM deficient cell lines and changes in expression or phosphorylation of Rad21 in these cell lines after exposure to a variety of DNA damaging agents. Human Rad21 appears to encode variable isoforms in different cell lines but there was no correlation of a specific isoform with ATM status.

4) Yue Wei, Department of Biochemistry; Mentor, Wade Harper, Ph.D., Professor; "Interactions of cyclin E, BRCA2 and NPAT in mammary cancer."

ABSTRACT

Cyclin E/CDK2 is the primary CDK complex regulating the onset of DNA replication in mammalian cells. It plays an important role in neoplasia. Also, overexpression of cyclin E is implicated in facilitating breast cancer progression. Various substances including proteins produced by oncogenic viruses affect cyclin E. To further elucidate the mechanism about how cyclin E/CDK2 regulates cell cycle, and how it is related to tumorigenesis and progression, we used the method of expression cloning to reveal a series of cyclin E/CDK2 interacting proteins. BRCA2 and NPAT are two of them that are of most interest. Human Brca2 is a tumor suppresser gene. Inherited mutations of BRCA2 and BRCA1 genes are found in about half of the familial breast cancer patients. Evidence suggests that Brca1 and Brca2 proteins have common biological functions, especially in DNA damage repair and cell cycle regulation. Brca1 is phosphorylated in response to DNA damage and cell cycle progression, especially by cyclin dependent kinase 2 (CDK2). Brca2 may also undergo hyperphosphorylation in part through CDK2. Indeed, there are potential RXL motifs and CDK phosphorylation sites in the C-terminal half of Brca2. A current goal is to test if cyclin E/CDK2 dependent phosphorylation of Brca2 plays a role in regulating DNA damage checkpoint in cell cycle. Aim 1 is to find out if Brca2 protein is phosphorylated by CDK2; if so, which part of Brca2 is phosphorylated. Aim 2 is to find out if the phosphorylation of Brca2 by CDK2 is RXL motif dependent. Aim 3 is to identify the phosphorylation sites on Brca2 by CDK2.

Progress in these aims include the following: A series of recombinant flag-tagged/GST-fused Brca2 fragments (N:1-1173, M:927-2612, C2:2184-2985, C1:2951-3418) have been expressed and purified from insect cell expression system; fragment N, C2 and C1 of Brca2 was found phosphorylated by cyclin E/CDK2 and cyclin A/CDK2 *in vitro*; phosphorylation of fragment C1 by CDK2 was reduced by an E2F peptide with RXL motif. Besides Brca2, the NPAT gene, which encodes a novel cell cycle regulating protein, has been studied. NPAT protein interacts with cyclin E and is phosphorylated by cyclin E/CDK2. It has been localized in cell cycle regulated nuclear foci. Preliminary data suggest that NPAT may play a role in histone gene transcription.

5) Geetika Chakravarty, Ph.D., Department of Molecular and Cellular Biology; Mentor, Jeffrey Rosen, Ph.D., Professor; "p190B in mammary development and cancer."

ABSTRACT

In addition to systemic hormones, local growth factors, stroma and the extracellular matrix (ECM), the ECM-signaling proteins also play a critical role in tissue remodeling during mammary gland development. Since p190-B has been shown to be directly involved in the regulation of the actin cytoskeleton, and, therefore, may influence mammary morphogenesis, the overall objective of this fellowship was to elucidate the role of p190-B during mammary gland development and in breast cancer.

In previous studies, p190-B has been shown to localize to focal adhesion plaques upon integrin clustering. Of additional interest is the report in which the activation of the ß1-integrin signaling was shown to stimulate tyrosine phosphorylation of $p190^{RhoGAP}$ and membrane-protrusive activities in invadopodia in melanoma cells. The biochemical activities of Rho-GTPases are thus crucial for modulating cytoskeletal architecture. p190-B is developmentally regulated during mammary development and interestingly was found to be overexpressed in a subset of murine mammary tumors by Northern blot analysis. Thus, p190-B may play a role in cell motility and in the invasion of TEB into the surrounding stroma and its aberrant expression may occur in rodent mammary tumors. In order to help elucidate the function of p190-B during virgin mammary development its pattern of expression in adult virgin mammary gland tissue was examined by *in situ* hybridization. The p190-B cDNA was linearized to generate an 800 – 900bp ^{33}P-labeled antisense riboprobe. ^{33}P-labeled probes exhibited less background than ^{35}S-probes, and were also of higher specific activity, which was necessary to detect rare transcripts. Since mammary gland stroma is known to give rise to considerable nonspecific background, the results were further confirmed by competing the ^{33}P labeled riboprobes with increasing concentration of unlabeled probe. In agreement with previous results, p190-B expression was highest in the highly proliferative outer layer of cells lining the TEB suggesting it may facilitate invasion of the TEB into the fat pad during ductal morphogenesis. Stroma, ducts and alveolar buds were all shown to express p190-B but at much reduced levels.

In order to better understand how p190-B may be implicated in signaling pathways regulating cell transformation and/or invasion, p190-B was transiently transfected into MCF-10A human mammary epithelial cells using an efficient adenovirus-mediated transfection protocol. The function of p190-B was assessed initially by analyzing actin stress fiber

organization in these cells grown on coverslips using FITC-Phalloidin staining. Eighty-four percent of p190-B-transfected cells exhibited a significantly reduced actin stress fiber network as compared to only 9% of the non-transfected cells. The staining pattern in the p190-B expressing cells was circumfrential as opposed to the fine overall network of actin stress fibers observed in non-transfected cells. In addition, the majority of p190-B-transfected cells exhibited a tendency to detach from the MCF-10A cell clusters, and remained as single, isolated cells (60%) or in pairs detached from the cell monolayer. p190-B expression in these transfected cells appeared punctate in the cytoplasm, and was not localized at focal adhesions as might be expected if these cells had been grown on an extracellular matrix. These studies suggest that p190-B over-expression results in disruption of the actin cytoskeleton, which may in turn make the cells less adherent, an important step in cell migration and invasion. Studies are in progress to use high titer retroviral vectors to introduce p190-B into MCF10A cells followed by measurement of their invasive potential using modified Boyden chamber assay. Three different types of high titer viruses are being tested to see which one of these transduces human MCF10A cells most efficiently.

In order to further define the biological function of p190-B *in vivo* and to investigate the potential consequence of ablating this gene on mammary development, a conditional knockout of the gene has been proposed. Although a genomic clone was available from Dr. Yamada, it did not contain sufficient 3' sequences to engineer the loxP sites for site-specific recombination. A 129SV/EV library was, therefore, successfully screened to obtain clones containing additional 3' sequence.

6) Xianshu Cui, Ph.D., Department of Molecular Virology and Microbiology; Mentor, Larry Donehower, Ph.D., Associate Professor; "Interactions of wnt-1 and tumor-suppressor genes."

ABSTRACT

The main goal of this research is to examine interactions of wnt-1 with tumor suppressor genes using transgenic/knockout mouse models and elucidate critical genes involved in these bigenic crosses. Three models are being examined. By crossing the wnt-1 transgenic mice to the p53 deficient mice, a mammary gland tumor model was established. Comparing the tumorigenesis of wnt-1 mice deficient of p53 to those retain wild type p53, a few biological differences were observed such as tumor growth and cell proliferation rate, and histopathology of tumor cells. To understand the molecular basis of the biological findings, the present study searches for genes that are differentially expressed in mammary gland tumor cells of Wnt-1 mice with different status of p53. With the methods of differential display and gene expression array, a dozen genes were identified. Ten of those differentially expressed genes were confirmed with either northern analysis or ribonuclease protection assay. Eight of the genes are higher expressed in p53 +/+ tumors, which include alpha-smooth muscle actin, kappa casein, Aldolase C, cytokeratin 19, KET, C-kit, p21 and Cyclin G1. Two genes were found higher expressed in p53-/- tumors that are Cyclin B1 and FGFR1iiib.

Chk1 gene is a DNA damage responsive gene primarily found in yeast. Chk1 gene has been implicated in cell cycle checkpoint control in lower eykaryotes. Dr. Elledge's Lab initiated the study for Chk1 gene function in mammals by setting up a mouse model with

targeted disruption of Chk-1. The results show that Chk-1 is essential for peri-implantation embryonic development; is required for cell cycle arrest at G2-M phase; is downstream of Atr in the DNA damage response. No enhancement of tumor growth is observed for Chk1 heterozygous mice up to 18 months old. Chk1-deficient mice were crossed with wnt-1 transgenic mice. Chk1 +/- mice developed mammary gland tumors earlier (5 weeks) than Chk1+/+ mice without accelerating the tumor growth rate. All of 9 tested Chk1 +/- tumors retained their wild allele of Chk1.

Brca-2 tumor suppressive function in human breast cancer is well established. Earlier study showed that Brca-2 null is lethal for mouse embryo development. Brca-2 heterozygous mouse did not show differences for tumor development compared to Brca-2 wild type mice. We crossed Brca-2 deficient mice with Wnt-1 transgenic mice. The results showed no differences between Brca-2 +/- and Brca-2 +/+ mice for both mammary gland tumor development and tumor growth rate.

c. Enhancement Programs

Three education programs specific for this training program were functional over the past year. The weekly "Breast" seminar included faculty and trainees. The schedule for the seminar series is shown in Table 1. Drs. Gould and Thorpe were invited speakers sponsored by the Baylor Breast Spore.

The second education enhancement program is the Invited Speakers program. This program allows both the faculty and fellows supported by the program to interact with the invited speaker. The two speakers were Dr. Kay-Uwe Wagner who spoke on the subject of conditional BRCA1 mouse model and Dr. John Wysolmerski who spoke on the subject of role of parathyroid hormone-related protein and mammary development.

The third education enhancement program is the course in "Molecular Carcinogenesis", which is given every Winter bloc and each predoctoral trainee is required to pass. This course is organized by Dr. Larry Donehower and the teaching faculty include Drs. Medina, Harper, Donehower and Butel.

d. Trainee Review

With respect to trainee review, there were two turnovers for the new year. Andrew Dennis was awarded an individual predoctoral fellowship from the USAMRC Breast Cancer Training Program. Amy Tabor finished her course work and received a MS degree and departed Baylor College of Medicine to pursue other opportunities. The prospective trainees to fill the two vacated positions were nominated by letter and supporting documentation, reviewed by a subcommittee of the participating training faculty and the successful applicants notified by letter that their respective fellowships would start July 1, 2000.

e. Reportable Outcomes

Two of the predoctoral trainees, Andrew Dennis and Yue Wei, attended national meetings. Andrew Dennis attended the 82nd Annual Meeting of the Endocrine Society and presented a poster entitled, "Characterization of Human UBA3: A Novel Type of Nuclear Hormone Receptor Coactivator." Yue Wei attended The Cold Spring Harbor Laboratory meeting entitled, "The Cell Cycle." Dr. Chakravarty's paper on "p190-B, a Rho-GTPase activating protein, is differentially expressed in terminal end buds and breast cancer" was accepted for publication in the journal *Cell Growth and Differentiation.* Dr. Cui was a co-author on the paper entitled, "Chk1 is an essential kinase that is regulated by *atr* and required for the G9(2)M DNA damage checkpoint," in the journal *Genes and Development 14*:1448-1459, 2000.

7. CONCLUSIONS

The training program in breast cancer is functioning as planned and major alterations are not planned at this time. The only minor change instituted for the forthcoming year is to include some faculty from the Baylor Breast Care Center as participating faculty, thus enabling these faculty to have students supported by the training grant. The inclusion of some of these faculty is a logical extension of their participation in our weekly Breast seminar and provides an important element in the total educational and training components of our program.

8. APPENDICES

a. Liu, Q., Guntuku, S., Cui, X.S., Matsuoka, S., Cortez, D., Tamai, K., Luo, G., Carattini-Rivera, S., DeMayo, F., Bradley, A., Donehower, L.A., and Elledge, S.J. Chk1 is an essential kinase that is regulated by *atr* and required for the G(2)/M DNA damage checkpoint. *Genes and Development 14*:1448-1459, 2000.

b. Chakravarty, G., Roy, D., Gonzales, M., Gay, J., Contreras, A., and Rosen, J.M. p190-B, a Rho-GTPase-activating protein, is differentially expressed in terminal end buds and breast cancer. *Cell Growth & Differentiation 11*:0000-0000, 2000 (*in press*).

Table 1. Breast Seminar
Wednesdays 12:00 p.m., Room M616 (Debakey Bldg.)
September 15, 1999 – June 16, 2000

DATE	NAME	TITLE	DEPARTMENT
9/15	Kent C. Osborne, Ph.D.	Professor	Medicine
9/22	Jeffrey M. Rosen, Ph.D.	Professor	Molecular & Cellular Biology
9/29	D. Craig Allred, M.D.	Professor	Pathology
10/6	Larry Donehower, Ph.D.	Assoc. Professor	Molecular Virology
10/13	Gary M. Clark, Ph.D.	Professor	Medicine
10/20	Ming Zhang, Ph.D.	Asst. Professor	Molecular & Cellular Biology
10/27	Susan Hilsenbeck, Ph.D.	Assoc. Professor	Medicine
11/03	Sharon E.Plon, M.D., Ph.D	Asst. Professor	Pediatric Hem/Onc & Genetics
11/10	Powell H. Brown, Ph.D.	Assoc. Professor	Medicine
11/17	J. Wade Harper, Ph.D.	Professor	Biochemistry
11/24	HOLIDAY		
12/01	Peter O'Connell, Ph.D.	Professor	Molecular & Cellular Biology
12/08	RESCHEDULED		
12/15	Kay-Uwe Wagner, Ph.D.	Invited Speaker	National Cancer Institute
12/22 – 01/05	HOLIDAY WEEKS		
01/12	Daniel Medina, Ph.D.-cancelled	Professor	Molecular & Cellular Biology
01/19	Rafael E. Herrera, Ph.D.-cancelled	Asst. Professor	Medicine
01/26	Allan Bradley, Ph.D.	Professor	Molecular Genetics
02/02	Richard Elledge, M.D.	Assoc. Professor	Medicine
02/09	Adrian Lee, Ph.D.	Asst. Professor	Medicine
02/16	John Wysolmerski, M.D.	Invited Speaker	Yale University
02/23	Steffi Oesterreich, Ph.D.	Asst. Professor	Medicine
03/01	Suzanne Fuqua, Ph.D.	Professor	Medicine
03/08	Raghu Sinha, Ph.D.	Asst. Professor	Molecular & Cellular Biology
03/15	Sophia Tsai, Ph.D.	Professor	Molecular & Cellular Biology
03/22	RESCHEDULED		
03/29	Peter M. Haney, M.D., Ph.D.	Asst. Professor	Pediatric-Neonatology
04/05	OFF – AACR		
04/12	Thenaa K. Said, Ph.D.	Asst. Professor	Molecular & Cellular Biology
04/19	HOLIDAY WEEK		
04/26	Lakshmi Sivaraman, Ph.D.	Instructor	Molecular & Cellular Biology
05/03	Torsten A. Hopp, Ph.D. - cancelled	Instructor	Medicine
05/10	Michael N. Gould, Ph.D.	Invited Speaker	University of Wisconsin
05/17	Philip E. Thorpe, Ph.D.	Invited Speaker	UT Southwestern Med. School
06/16	James D. Marks, M.D., Ph.D.	Invited Speaker	Univ. of Calif., San Francisco

Chk1 is an essential kinase that is regulated by Atr and required for the G_2/M DNA damage checkpoint

Qinghua Liu,[1-3] Saritha Guntuku,[1,2] Xian-Shu Cui,[4] Shuhei Matsuoka,[1,2] David Cortez,[1,2] Katsuyuki Tamai,[7] Guangbin Luo,[1,5] Sandra Carattini-Rivera,[1,5] Francisco DeMayo,[6] Allan Bradley,[1,5] Larry A. Donehower,[4,6] and Stephen J. Elledge,[1,2,5,8]

[1]Howard Hughes Medical Institute, [2]Verna and Marrs McLean Department of Biochemistry, [3]Program in Cell and Molecular Biology, [4]Department of Molecular Virology and Microbiology, [5]Department of Molecular and Human Genetics, and [6]Department of Molecular and Cellular Biology, Baylor College of Medicine, Houston, Texas 77030 USA; [7]Medical and Biological Laboratories Co., Ltd., Ina, Nagano 396-0002, Japan

Chk1, an evolutionarily conserved protein kinase, has been implicated in cell cycle checkpoint control in lower eukaryotes. By gene disruption, we show that *CHK1* deficiency results in a severe proliferation defect and death in embryonic stem (ES) cells, and peri-implantation embryonic lethality in mice. Through analysis of a conditional *CHK1*-deficient cell line, we demonstrate that ES cells lacking Chk1 have a defective G_2/M DNA damage checkpoint in response to γ-irradiation (IR). *CHK1* heterozygosity modestly enhances the tumorigenesis phenotype of *WNT-1* transgenic mice. We show that in human cells, Chk1 is phosphorylated on serine 345 (S345) in response to UV, IR, and hydroxyurea (HU). Overexpression of wild-type Atr enhances, whereas overexpression of the kinase-defective mutant Atr inhibits S345 phosphorylation of Chk1 induced by UV treatment. Taken together, these data indicate that Chk1 plays an essential role in the mammalian DNA damage checkpoint, embryonic development, and tumor suppression, and that Atr regulates Chk1.

[*Key Words*: Atr; Atm; Chk1; embryonic lethality; DNA damage; checkpoint]

Received March 20, 2000; revised version accepted May 1, 2000.

The ability of organisms to sense and respond to DNA damage is critical for their long-term survival. Consequently, cells have evolved an elaborate DNA damage response pathway that senses aberrant DNA structures and transmits a damage signal to effectors that act to enhance survival of the organism (Elledge 1996). Activation of the DNA damage response pathway results in transcriptional induction of genes involved in DNA repair, activation of DNA repair pathways, and arrest of cell cycle progression. In metazoans, cells experiencing DNA damage may also undergo apoptotic cell death, thereby preventing these cells from possibly contributing to tumorigenesis or other diseases. Because many genes involved in the regulation of DNA damage responses were originally identified based on their ability to control cell cycle progression, the DNA damage response pathway is also often referred to as the DNA damage checkpoint pathway.

The mammalian DNA damage response pathway consists of several families of conserved protein kinases. Two members of the phosphoinositol kinase (PIK) family, Atm and Atr, are at the top of this signal transduction cascade. Although related, Atm and Atr form two distinct subfamilies in evolution. Atm is more closely related to Tel1 in *Saccharomyces cerevisiae* and *Schizosaccharomyces pombe*, whereas Atr (Cimprich et al. 1996; Keegan et al. 1996) is more closely related to Mec1 in *S. cerevisiae*, Rad3 in *S. pombe*, and Mei-41 in *Drosophila melanogaster* (for review, see Elledge 1996). The *ATM* gene is mutated in the familial neural degeneration and cancer-predisposition syndrome ataxia telangiectasia (Savitsky et al. 1995). *ATM* deficient mice are viable, but show growth retardation, infertility, and cancer predisposition (Barlow et al. 1996; Xu et al. 1996). *ATM* mutant cells are defective for DNA damage checkpoints and are very sensitive to agents that cause double-stranded DNA breaks, such as γ-irradiation (IR). Like *ATM* mutant cells, yeast *tel1* mutants have short telomeres, but they have intact cell cycle checkpoints and display only limited sensitivity to DNA-damaging agents. Less is known about Atr due to a lack of *ATR* mutant cells. However, overexpression of a kinase-defective Atr mutant abrogates cell cycle arrest after DNA damage, revealing a role in DNA damage checkpoints (Cliby et al. 1998; Wright et al. 1998). *ATR* disruption in mice results in peri-implantation embryonic lethality and fragmented chromosomes (Brown and Baltimore 2000). In *D. melanogaster*, *mei-41* mutant embryos cannot properly lengthen the cell cycle at the midblastula

[8]Corresponding author.
E-MAIL selledge@bcm.tmc.edu; FAX (713) 798-8717.

transition and this leads to embryonic lethality (Sibon et al. 1999).

Downstream of Atm and Atr are two families of protein kinases, Chk1 and Chk2. The Chk2 family consists of Rad53 in *S. cerevisiae* and Cds1 in *S. pombe* (for review, see Elledge 1996), and Chk2/Cds1 in mouse and human (Matsuoka et al. 1998; Blasina et al. 1999; Brown et al. 1999; Chaturvedi et al. 1999). The Chk2 family kinases can be activated by DNA damage or replication blocks and this activation requires upstream PIK members in their respective species (Sanchez et al. 1996; Sun et al. 1996; Boddy et al. 1998; Lindsay et al. 1998). Chk2 is involved in DNA damage checkpoints because Chk2-deficient embryonic stem (ES) cells fail to maintain G_2 arrest after DNA damage (Hirao et al. 2000). *CHK2*$^{-/-}$ thymocytes are resistant to IR-induced apoptosis and fail to stabilize and activate p53 in response to IR (Chehab et al. 2000; Hirao et al. 2000).

The Chk1 kinase family consists of Chk1 in *S. pombe* (Walworth et al. 1993; Al-Kohairy et al. 1994), *S. cerevisiae* (Sanchez et al. 1999), and *Xenopus laevis* (Kumagai et al. 1998) and *grapes* in *D. melanogaster* (Fogarty et al. 1997; Sibon et al. 1997; Su et al. 1999). In *S. cerevisiae*, Chk1 controls the pre-anaphase arrest after DNA damage by preventing degradation of Pds1, an inhibitor of anaphase entry (Sanchez et al. 1999). In *S. pombe* and *Xenopus*, Chk1 is required for the G_2 arrest induced by DNA damage, and in *Xenopus* for the prophase I arrest of oocytes (Nakajo et al. 1999). In *S. pombe*, Chk1 is phosphorylated in response to DNA damage in a Rad3-dependent manner and this is accompanied by an increase in 14-3-3 protein association (Walworth and Benards 1996; Chen et al. 1999). In *D. melanogaster*, *grapes* mutants display an embryonic lethal phenotype similar to that of *mei-41* mutants. Although the phenotype of *mei-41* and *grapes* mutants is complex, at least part of the defects is likely to be attributed to premature entry of mitosis.

Less is known about Chk1 function in mammals. In human cells, Chk1 is shown to be phosphorylated in response to IR and thus, is implicated in the DNA damage response pathway (Sanchez et al. 1997). Because yeast and human Chk1 can phosphorylate Cdc25C in vitro on the inhibitory phosphorylation site S216, Chk1 may function as an effector of the DNA damage checkpoint that activate G_2 arrest by inhibiting Cdc2 kinase activities through Cdc25C. It is currently unclear, however, which PIK members are the regulators of Chk1 in mammalian cells. Thus, we generated a *CHK1* knockout mouse and subsequently, a conditional *CHK1*-deficient ES cell line. Our results indicate that Chk1 is regulated by Atr and plays a crucial role in the G_2/M DNA damage checkpoints, embryonic development, and tumor suppression. A model concerning the mammalian DNA damage response pathway will also be discussed.

Results

Generation of a Chk1 knockout mouse

We disrupted the *CHK1* gene in murine ES cells by gene targeting. The targeting vector consists of a *neo* marker for positive selection flanked by 1.9 kb and 4.5 kb of *CHK1* homologous sequences, and a *TK* marker for negative selection (Fig. 1A). Homologous recombination with this targeting vector removes 3 kb of *CHK1* genomic sequence, including exons 2–5 that encode the putative first methionine, the "GxGxxG" ATP-binding motif and half of the kinase domain. Thus, it is likely to generate a null allele. Eight Chk1 heterozygous ES clones were obtained from screening 192 G418- and FIAU-resistant colonies (Fig. 1B). Four independent cell lines were injected to generate chimeras, of which three produced germ-line transmission. The phenotype, as described below, was consistent among all different lines.

Chk1 deficiency results in peri-implantation lethality

CHK1 heterozygous mice are healthy, fertile, and tumor-free up to 1.5 years of age. However, when the heterozygous mice were intercrossed, no *CHK1* homozygous mice were detected among 139 offspring, indicating that Chk1 deficiency results in embryonic lethality. Systematic analysis of embryonic day 6.5 (E6.5)–E15.5 embryos generated from heterozygotes matings failed to detect *CHK1* null embryos at any stage examined (data not shown). Empty decidua and remains of resorbed embryos were often observed at E6.5 or E7.5 in heterozygotes intercross, but were rarely seen in backcross between heterozygous and wild-type mice (Fig. 1C; data not shown). These results suggest that the lethality of *CHK1* null embryos may occur before E6.5.

Therefore, we isolated and cultured blastocysts from intercrossed *CHK1* heterozygous females at E3.5. PCR genotyping of newly isolated blastocysts revealed that the fraction of *CHK1* null embryos was always between one-seventh and one-sixth, well below the predicted one-quarter Mendelian ratio. And these null embryos often displayed abnormal morphology distinctive from their wild-type or heterozygous littermates (data not shown). When these blastocysts were cultured in vitro up to 7 days, the majority would continue to proliferate, hatch from the zona pellucida on the first or second day in culture, and immediately attach or "implant" to the Petri dish surface (Fig. 2A). The trophoectoderm of blastocysts spread into a single cell layer and divided a few times before terminally differentiating into giant trophoblast cells. Above the trophoblast cells lay the inner cell mass (ICM), which continued to proliferate to generate a large cell mass. These proliferating blastocysts, by genotyping, consisted of only wild type and heterozygotes with a 1:2 ratio. In contrast, a small group of blastocysts would stop proliferation, fail to hatch, and degenerate inside the zona pellucida (Fig. 2A). These nonproliferative blastocysts were presumably the missing homozygous mutant embryos, however, their genotype could not be confirmed by PCR due to massive DNA fragmentation during embryo degeneration. Three mutant blastocysts hatched on the third or fourth day in culture, laying down a few trophoblast cells but no ICM. We obtained the genotype of two of these embryos and both were *CHK1*$^{-/-}$. These results suggested that *CHK1*$^{-/-}$

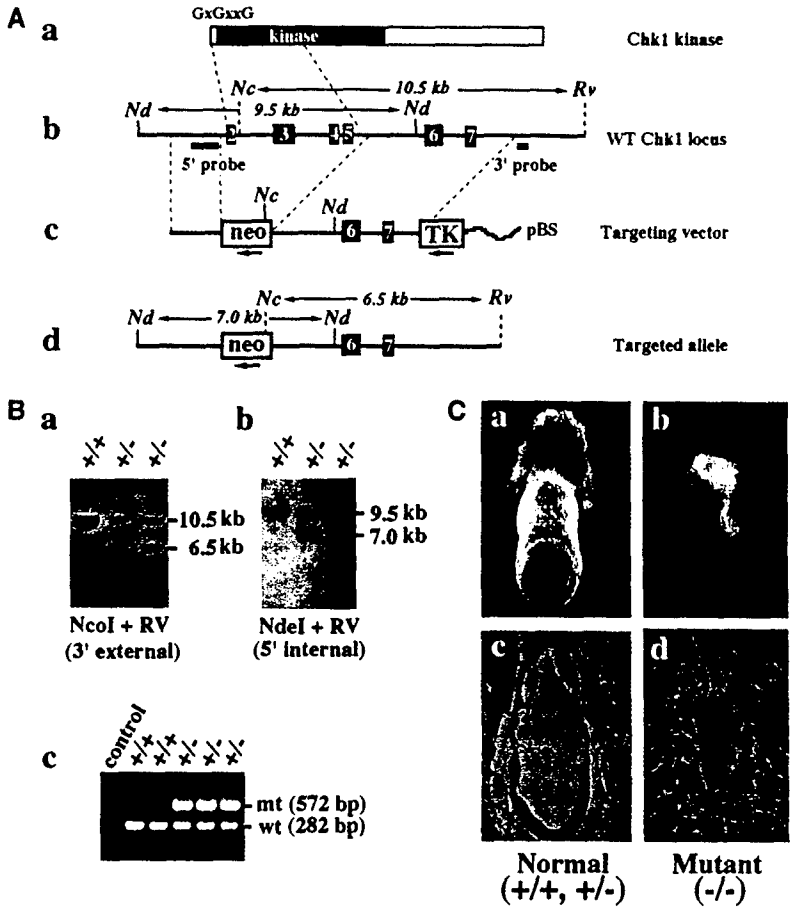

Figure 1. *CHK1* disruption results in early embryonic lethality. (*A*) Disruption of the *CHK1* gene in ES cells. (*a*) Chk1 protein structure. Located at the amino terminus are the "GxGxxG" ATP-binding motif and kinase domain. (*b*) Restriction map of the wild-type *CHK1* locus including exons 2–7 and location of the 3′ external and 5′ internal probes used for Southern blots shown below. (*c*) Restriction map of the *neo* targeting vector. The direction of transcription is shown by arrows beneath the *neo* and *TK* markers. (pBS) pBluescript plasmid. (*d*) Predicted restriction map of the targeted *CHK1* allele. Only relevant restriction sites are shown. (*Nc*) *Nco*I; (*Nd*) *Nde*I; (*Rv*) *Eco*RV. (*B*) Identification of $CHK1^{+/-}$ ES clones by Southern blot analysis. (*a*) Genomic DNA was digested with *Nco*I and *Eco*RV and probed with the 3′ external probe. Genotypes are shown above each lane. $CHK1^{+/-}$ ES clones showed a 10.5-kb wild-type and a 6.5-kb mutant band as predicted. (*b*) Genomic DNA was digested with *Nde*I and probed with the 5′ internal probe. $CHK1^{+/-}$ ES clones displayed a 9.5-kb wild-type and a 7.0-kb mutant band. (*c*) *CHK1* genotyping by PCR. The wild-type and mutant *CHK1* alleles generate a 282-bp and a 572-bp band, respectively. (*C*) Morphological and histological analysis of E7.5 embryos isolated from $CHK1^{+/-}$ intercrosses. A typical photograph is shown for normal (*a*,*c*) and mutant (*b*,*d*) E7.5 embryos freshly dissected from decidua (*a*,*b*) or hematoxylin and eosin-stained sections of E7.5 decidua (*c*,*d*).

blastocysts have a proliferation defect and that Chk1 may be required for proliferation or survival of early embryonic cells.

Because less than one-quarter of blastocysts were homozygotes and they often displayed abnormal morphology, we examined eight-cell morula isolated from intercrossed $CHK1^{+/-}$ females at E2.5. PCR genotyping revealed the predicted 1:2:1 ratio of $CHK1^{+/+}$:$CHK1^{+/-}$:$CHK1^{-/-}$ embryos at the eight-cell stage (Fig. 2C; data not shown). When these morula were cultured in vitro, it was found that $CHK1^{-/-}$ embryos developed normally until the early blastocyst stage; however, unlike the wild-type and heterozygous littermates, they failed to continue proliferation or hatch and subsequently degenerated inside the zona pellucida (Fig. 2B). These in vitro embryo culture experiments suggest that Chk1 deficiency results in peri-implantation embryonic lethality.

CHK1 deficient embryos die of p53-independent apoptosis

To determine whether *CHK1*-deficient embryos were dying of apoptosis, we isolated eight-cell morula at E2.5 and allowed them to develop in vitro into early stage blastocysts. We then used these blastocysts to perform terminal deoxynucleotide end-labeling (TUNEL) assays that fluorescently labels the ends of fragmented DNA, a hallmark of apoptotic cells. Although wild-type and heterozygous littermates normally showed two to four fluorescent dots, *CHK1* homozygous blastocysts displayed many fluorescent dots, indicative of massive apoptosis (Fig. 2D). To further confirm the TUNEL results, we stained these embryos with 4,6-diamidino-2-phenylindole (DAPI) and observed them under the confocal microscope. Indeed, many cells in $CHK1^{-/-}$ embryos had condensed and fragmented nuclei that is characteristic of apoptosis (Fig. 2E). These results suggest that *CHK1*-deficient embryos die of apoptosis at the blastocyst stage.

To determine whether p53 is responsible for the apoptosis observed in blastocysts, we mated $p53^{-/-}$ $CHK1^{+/-}$ male and female mice, which is expected to generate $p53^{-/-}$ mice with $CHK1^{+/+}$, $CHK1^{+/-}$, and $CHK1^{-/-}$ genotype with a 1:2:1 ratio. Eight-cell morula were isolated from these intercrosses at E2.5, cultured for 2 days and picked for the TUNEL assay. The p53 null mutations could neither rescue nor delay the early lethality of $CHK1^{-/-}$ embryos (data not shown). Furthermore, $CHK1^{-/-}$ $p53^{-/-}$ blastocysts underwent apoptosis to the same degree as $CHK1^{-/-}$ blastocysts, suggesting that the apoptosis is independent of p53.

Chk1 is essential for ES cell viability

To investigate the function of Chk1 at the cellular level, we attempted to generate $CHK1^{-/-}$ ES cells by sequential

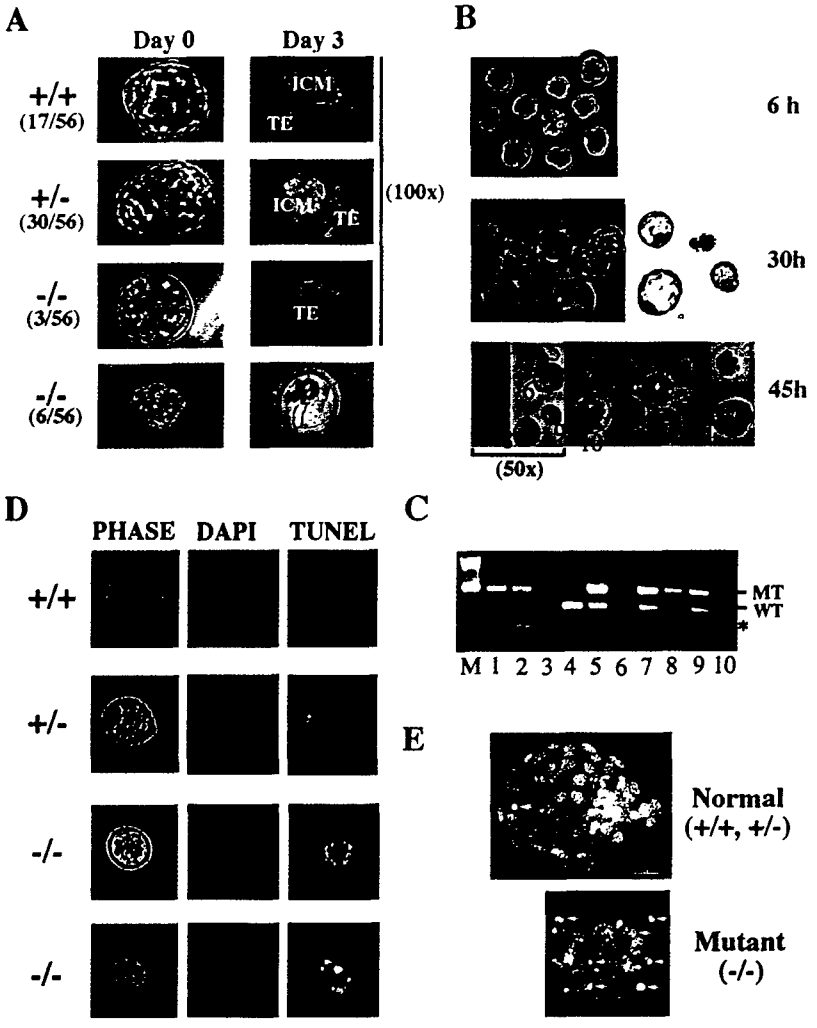

Figure 2. In vitro culture of preimplantation embryos. (*A*) In vitro culture of blastocysts isolated from $CHK1^{+/-}$ intercrosses. A typical image at day 0 and day 3 are shown along with the percentage of each category. (TE) Trophoectoderm; (ICM) inner cell mass. All images are 320× except when otherwise indicated. (*B*) In vitro culture of eight-cell morula. Shown here are a litter of 10 embryos isolated from a $CHK1^{+/-}$ intercross. The images were captured at 6, 30, and 45 hr in culture (100× except when otherwise indicated). The asterisks indicate the empty zona pellucida after the embryos have hatched. The embryos were individually picked and labeled 1–10. Embryos 1, 2, 3, and 10 failed to hatch. (*C*) PCR genotyping of embryos from *B*. The lane numbers correspond to that of the embryos. Embryo 6 was lost during transfer and embryo 3 was too degenerate to give any products. (WT) Wild type; (MT) mutant. The asterisk indicates a nonspecific band generated by primers alone. (*D*) TUNEL analysis of blastocysts derived as described in *B* (100×). (*E*) Confocal images (DAPI, 1000×) of blastocysts analyzed in *D*. The arrows indicate condensed and fragmented nuclei.

gene targeting. A second targeting vector containing the *hprt* marker was constructed and used to transfect $CHK1^{+/-}$ ES cells, in which one *CHK1* allele was disrupted previously by *neo*. When selected for both markers, no targeting event could be obtained from 384 G418/HAT/FIAU-resistant colonies. When selected only for *hprt*, 18 targeted clones were obtained after screening 351 HAT/FIAU-resistant colonies and in all cases the *hprt* construct had replaced the *neo*-disrupted mutant allele instead of the wild-type gene (data not shown). These results suggest that Chk1 is probably essential for proliferation or survival of ES cells.

Therefore, we constructed conditional *CHK1*-deficient ES cells by flanking the second exon of one *CHK1* allele with *loxP* sites and disrupting the other by gene targeting (Fig. 3A,B). This *lox*-flanked (flox) *CHK1* allele can be converted into a null allele after excision of exon 2 by Cre–*lox* site-specific recombination because it contains the translational initiation sequence and encodes the ATP-binding site for the kinase. When three independent $CHK1^{flox/-}$ cell lines were transfected transiently with a *CMV:Cre* plasmid, no excised clones were detected by Southern blot analysis among total of ~400 ES colonies (data not shown). However, when a control $CHK1^{flox/+}$ cell line was transfected with *CMV:Cre*, 28% (25 of 88) of the colonies underwent 100% excision, whereas an additional 10% (9 of 88) underwent partial or postmitotic excision, generating chimeric colonies (data not shown). These results confirm our prediction that excision of exon 2 from the *CHK1* gene generates a null allele, and are consistent with the previous finding that Chk1 plays an essential role in ES cells. Furthermore, the lack of chimeric excised colonies for Cre-transfected $CHK1^{flox/-}$ cells suggests that the defects associated with $CHK1^{-/-}$ cells are cell-autonomous and cannot be rescued by mixing with wild-type cells.

The absence of $CHK1^{-/-}$ colonies could theoretically be explained by an inability of the $CHK1^{flox/-}$ cells to excise or by cell death after the excision. To distinguish these two possibilities, we transfected both $CHK1^{flox/+}$ and $CHK1^{flox/-}$ ES cells with a *PGK:Cre* plasmid by electroporation and harvested cells after 24, 48, 72, and 96 hr. Southern blot analysis revealed that $CHK1^{flox/-}$ cells underwent excision as efficiently as $CHK1^{flox/+}$ cells (Fig. 3C, cf. lanes 2,3 with lanes 6,7). The excised and nonexcised cells were represented by the 7.5-kb and 5.1-kb band, respectively. Judging by their relative intensities, we estimated that ~60%–70% of cells underwent flox

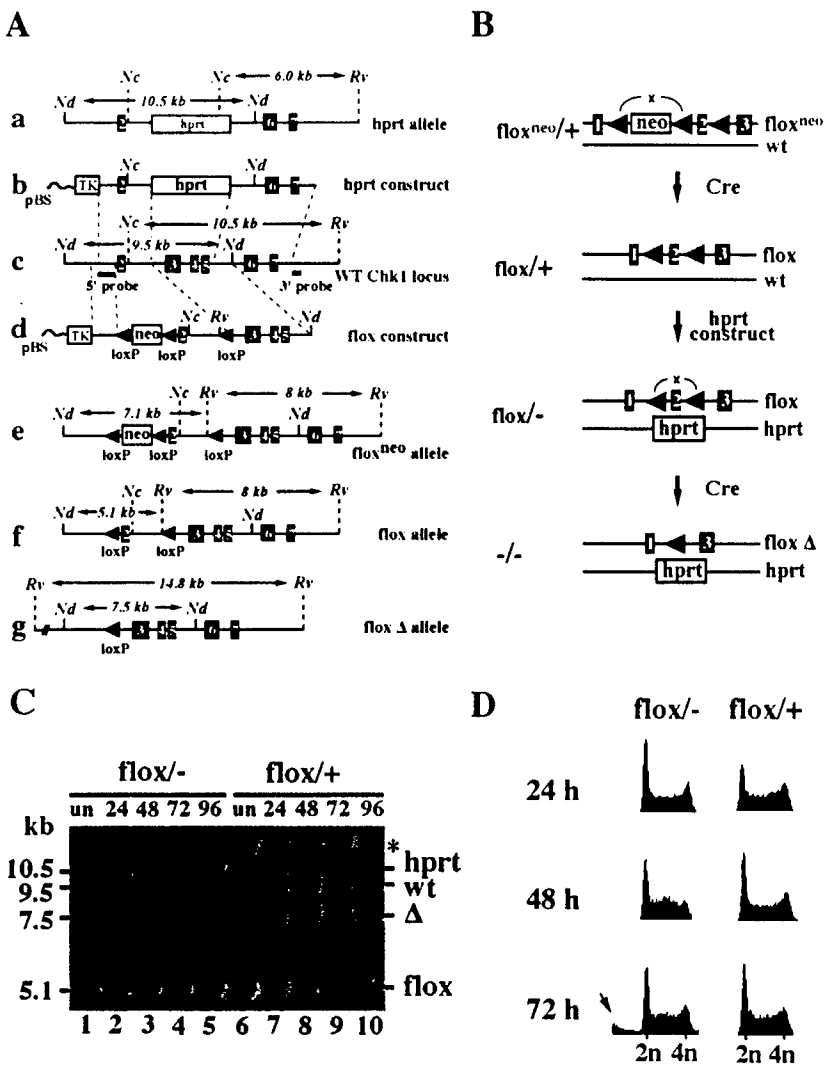

Figure 3. Construction and analysis of a conditional *CHK1*-deficient ES cell line. (*A*) Restriction maps of targeting vectors and targeted alleles. (*a*) *hprt* targeted allele; (*b*) *hprt* targeting vector; (*c*) wild-type *CHK1* locus; (*d*) flox targeting vector; (*e*) flox^{neo}-targeted allele; (*f*) flox allele generated after *neo* excision; (*g*) flox Δ allele generated after excision of exon 2. Only relevant restriction sites are shown. (*Nc*) *Nco*I; (*Nd*) *Nde*I; (*Rv*) *Eco*RV. (*B*) A schematic representation of the construction of conditional *CHK1*-deficient ES cells. In brief, a *CHK1* flox^{neo}/+ cell line was first obtained using the flox-targeting vector followed by the Cre–*lox*P-mediated *neo* excision to create *CHK1*$^{flox/+}$ cells. The remaining wild-type gene was then disrupted in the *CHK1*$^{flox/+}$ cells by the *hprt* targeting vector to generate *CHK1*$^{flox/-}$ cells. Finally, *CHK1*$^{flox/-}$ cells were conditionally converted into *CHK1*$^{-/-}$ cells by excision of exon 2 by transient transfection of *PGK:Cre*. (*C*) A Southern blot showing excision of the flox allele in *CHK1*$^{flox/+}$ and *CHK1*$^{flox/-}$ cells. Both are sister cell lines obtained from the same screen for generating *CHK1*$^{flox/-}$ cells. The asterisk refers to a band produced by random integration of the *hprt* construct in the *CHK1*$^{flox/+}$ cells. Genomic DNA was prepared from untransfected (lanes *1,6*) or Cre-transfected cells (lanes *2–5* and *7–10*) collected at 24, 48, 72, and 96 hr after electroporation, digested with *Nde*I and *Eco*RV and probed with the 5′ internal probe. Δ refers to the excised flox allele. The faint wild-type band present in lanes *2–4* was contributed by the feeder cells. (*D*) Comparison of Cre-transfected *CHK1*$^{flox/+}$ and *CHK1*$^{flox/-}$ cells by FACS (DNA content) analysis. Cells were harvested at 24, 48, and 72 hr after electroporation and stained with propidium iodide (PI). The arrow indicates cells with less than 2N DNA content that were present in the 72-hr flox/– sample.

excision in both cell lines by 48 hr after Cre transfection (Fig. 3C, lanes 3,8). However, although the excised flox/+ cells divided as fast as the nonexcised cells, the excised flox/– cells disappeared from the culture between 72 and 96 hr (Fig. 3C, cf. lanes 4,5 and lanes 9,10). Analysis of DNA content by FACS revealed a significant sub-G_1 population, which is characteristic of apoptotic cells, in the Cre-transfected *CHK1*$^{flox/-}$ cells at 72 hr after transfection (Fig. 3D). These results indicate that *CHK1*$^{-/-}$ cells have a severe proliferation defect accompanied by apoptotic death.

CHK1$^{-/-}$ *cells are defective for the* G_2*/M DNA damage checkpoint*

IR induces a predominant G_2 arrest in mouse ES cells (Aladjem et al. 1998; Hirao et al. 2000). To determine whether Chk1 is required for this G_2 arrest, we subjected *CHK1*$^{flox/-}$ ES cells to 10 Gy of IR at 24 hr after transfection with a *PGK:Cre* or a *CMV:GFP* plasmid. Twelve hours after irradiation, ~70%–80% of all cell types arrested at G_2 with a 4N DNA content, as measured by FACS analysis (Fig. 4A). However, at later time points the G_2-arrested population of *CHK1*$^{flox/-}$ cells declined, whereas the G_1–S population increased to 43.7% (18 hr) and 53.9% (24 hr), as more cells were converted to *CHK1*$^{-/-}$ cells (Fig. 4A). In contrast, all the control cells remained predominantly arrested at G_2. These results suggest that *CHK1*$^{-/-}$ cells may lack a functional G_2/M DNA damage checkpoint.

To determine whether *CHK1*$^{-/-}$ cells enter mitosis in the presence of DNA damage, we took advantage of the fact that mouse ES cells have a functional spindle checkpoint (Hirao et al. 2000). Cells were irradiated as described above and immediately placed in media containing nocodazole that will disrupt spindles and trigger a mitotic arrest. Twelve hours after IR and nocodazole treatment, 90% of all cell types arrested with a 4N DNA

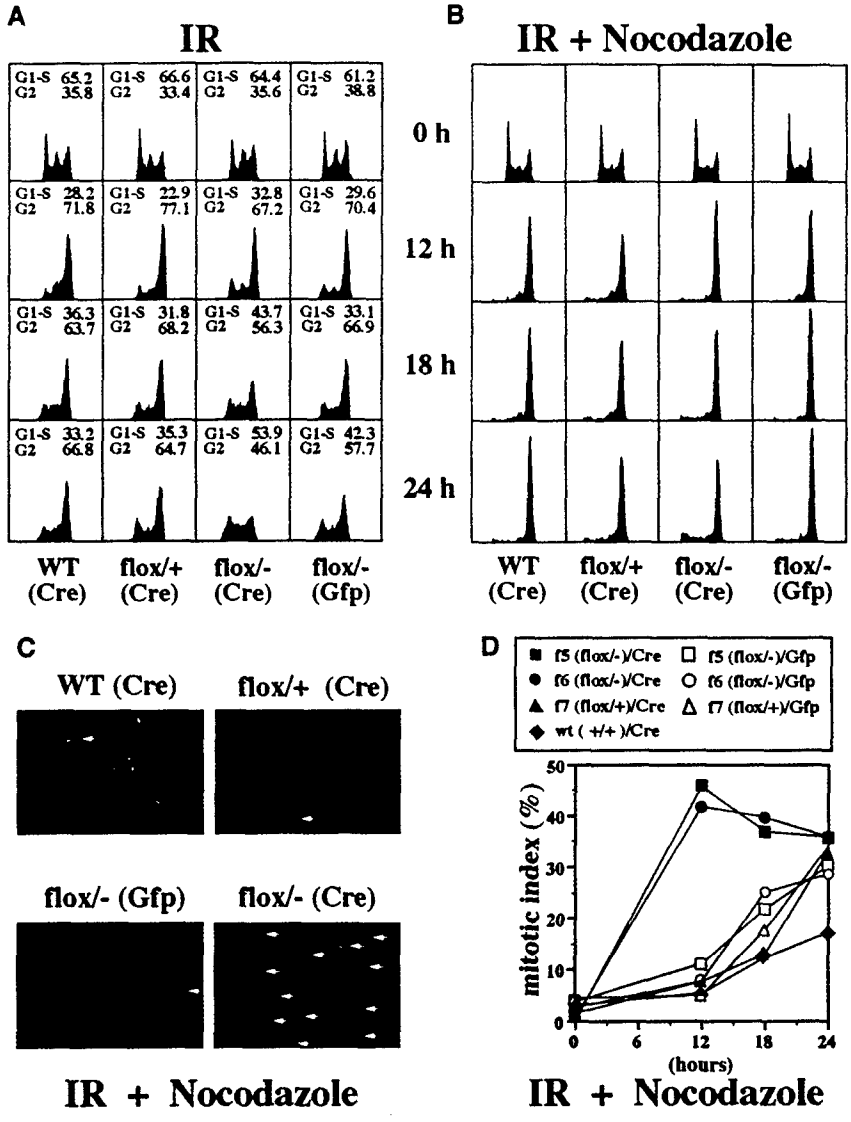

Figure 4. *CHK1*$^{-/-}$ cells are defective for the G_2/M DNA damage checkpoint. (*A*) FACS (DNA content) analysis of irradiated GFP- or Cre-transfected *CHK1*$^{+/+}$, *CHK1*$^{flox/+}$, and *CHK1*$^{flox/-}$ cells. Twenty-four hours after transfection, cells were subjected to 10 Gy IR, harvested at 0, 12, 18, and 24 hr and stained with PI. The percentage of G_1–S and G_2 population (mitotic cells are included in the G_2 counts but are generally a small proportion) is shown above each FACS sample. (*B*) FACS (DNA content) analysis of IR and nocodazole-treated cells. Cells of the indicated genotypes were transfected and irradiated as in *A* and incubated in nocodazole (0.2 μg/ml) containing media 30 min after irradiation. (*C*) Images (1000×) of the DAPI-stained 12-hr samples in *B*. Arrows indicate mitotic cells with condensed chromosomes and no nuclear membrane. (*D*) A mitotic index graph of IR and nocodazole-treated cells described in *B* and *C*. Cells (250–300) were counted for each sample. GFP or Cre transfections are indicated by open or closed circles. f5 and f6 represent two independent *CHK1*$^{flox/-}$ cell lines and f7 is a control *CHK1*$^{flox/+}$ cell line.

content as measured by FACS analysis (Fig. 4B). However, 40%–45% of Cre-transfected *CHK1*$^{flox/-}$ cells entered mitosis, in contrast to only 5%–8% of mitotic cells in GFP-transfected *CHK1*$^{flox/-}$ cells or Cre-transfected *CHK1*$^{+/+}$ and *CHK1*$^{flox/+}$ control cells (Fig. 4C,D). Because 60%–70% of *CHK1*$^{flox/-}$ cells are converted into *CHK1*$^{-/-}$ cells after *PGK:Cre* transfection, we estimate that at least 60% of *CHK1*$^{-/-}$ cells prematurely enter mitosis in spite of DNA damage. Thus, Chk1 is a bona fide component of the mammalian G_2/M DNA damage checkpoint. Furthermore, in response to DNA damage, the rapid kinetics and degree of inappropriate mitotic entry for *CHK1*$^{-/-}$ cells suggest that Chk1 is required for the initiation of G_2 arrest in response to DNA damage.

CHK1 *heterozygosity modestly enhances tumorigenesis of* WNT-1 *transgenic mice*

Examination of *CHK1*$^{+/-}$ animals up to the age of 18 months failed to detect a predisposition to early tumorigenesis. To determine whether reduction of *CHK1* dosage could enhance tumor formation in the context of other oncogenic stimuli, we crossed *CHK1*$^{+/-}$ mice to *WNT-1* transgenic mice, which contain a *WNT-1* oncogene driven by a mammary gland-specific mouse mammary tumor virus promoter (Tsukamoto et al. 1988). The *WNT-1* transgenic females develop early mammary gland hyperplasia and subsequent mammary adenocarcinomas at the ages of 3–12 months. Previous crosses of p53- and p21-deficient mice to *WNT-1* transgenic mice have revealed synergistic enhancements of tumor incidence or tumor growth rates in the bitransgenic offspring (Donehower et al. 1995; Jones et al. 1999). After the *WNT-1* transgenic/*CHK1*$^{+/-}$ crosses, we monitored 22 *CHK1*$^{+/-}$ *WNT-1* transgenic females and 22 *CHK1*$^{+/+}$ *WNT-1* transgenic females for tumors of the mammary gland. *CHK1*$^{+/-}$ females showed an earlier onset of mammary tumors compared to the *CHK1*$^{+/+}$ females (Fig. 5). The average age of tumor formation in the *CHK1*$^{+/-}$ mice was 168 days versus 219 days for *CHK1*$^{+/+}$ mice.

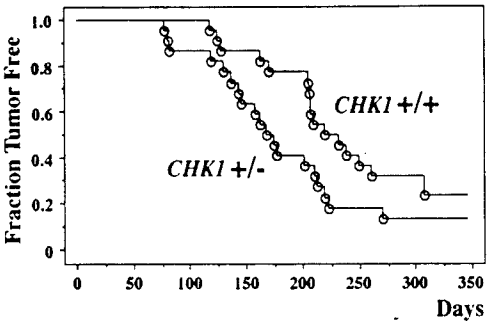

Figure 5. Kaplan-Meier plot of tumor incidence in *CHK1*$^{+/+}$ and *CHK1*$^{+/-}$ *WNT-1* transgenic females. Twenty-two animals of each genotype were monitored for mammary tumor formation for ~10 months. Tumor-free survival is plotted against the animal age in days.

Statistical comparison of the tumor incidence curves by the log-rank test, the Breslow-Gehan-Wilcoxon test, and the Peto-Peto-Wilcoxon test gave *P* values of 0.055, 0.030, and 0.030, respectively. These test scores indicate that the differences in tumor incidence between the *CHK1*$^{+/+}$ and *CHK1*$^{+/-}$ mice are marginally significant at the 0.05 level.

Further comparison of the *CHK1*$^{+/+}$ and *CHK1*$^{+/-}$ mammary adenocarcinomas revealed no obvious differences in gross pathology, histopathology, or growth rates. To assess whether the remaining wild-type *CHK1* allele was lost in the *CHK1*$^{+/-}$ tumors, we analyzed genomic DNA isolated from *CHK1*$^{+/-}$ tumors by Southern blot analysis. Of nine tumors examined, all nine retained an intact wild-type *CHK1* allele (data not shown), suggesting that reduction of *CHK1* dosage by 50% has a modest tumor-enhancing effect in the *WNT-1* transgenic model. The retention of the wild-type *CHK1* allele in the tumors is consistent with the finding that complete absence of Chk1 protein leads to cell lethality.

In vivo phosphorylation of Chk1 on S345 by Atr after DNA damage

In human cells, Chk1 is phosphorylated in response to DNA damage (Sanchez et al. 1997). Because SQ sites are known substrates of Atm and Atr (Banin et al. 1998; Canman et al. 1998), we raised rabbit polyclonal antibodies to peptides containing phosphorylated serine in the conserved SQ sites in human Chk1 protein. Only the anti-phospho-S345 (anti-p-S345) antibodies produced a signal specific for the phospho–antigen-peptide. Chk1 was immunoprecipitated with anti-Chk1 or anti-p-S345 antibodies from lysates prepared from 293T cells that were either untreated or treated with hydroxyurea (HU), UV, or IR. Although the anti-Chk1 antibodies brought down equivalent amounts of Chk1 proteins from all cell lysates, the anti-p-S345 antibodies immunoprecipitated Chk1 proteins only from HU-, UV-, or IR-treated cells, but not from untreated cells (Fig. 6A). This experiment suggests that in human cells Chk1 is phosphorylated on S345 in response to DNA damage or replication blocks.

Because *ATR* and *CHK1* disruptions both lead to periimplantation embryonic lethality in mice, we asked whether Atr regulates Chk1 in response to DNA damage. By transient transfection experiments, we showed that overexpression of wild-type Atr, but not the kinase-defective mutant Atr, increases the phosphorylation of co-transfected Chk1 on S345 in response to UV (Fig. 6B). Furthermore, overexpression of the kinase-defective mutant Atr in an inducible cell line (Cliby et al. 1998) inhibits the UV-induced S345 phosphorylation of endogenous Chk1 (Fig. 6C). These results suggest that Atr functions upstream of Chk1 in the mammalian DNA damage response pathway and is a major regulator of Chk1 phosphorylation after DNA damage.

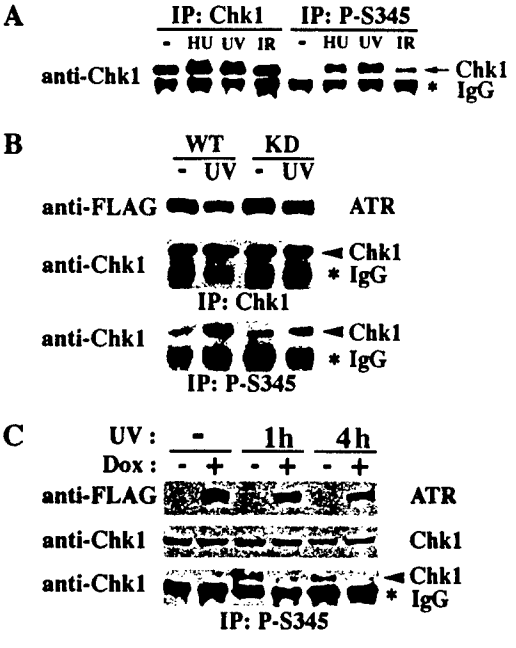

Figure 6. Chk1 is phosphorylated on S345 after DNA damage and this is regulated by Atr. (*A*) Phosphorylation of Chk1 on S345 after DNA damage. 293T cells were untreated or treated with IR (20 Gy and harvested after 1 hr), UV (50 J/m^2 and harvested after 2 hr) or HU (1 mM for 24 hr). Whole cell lysates were immunoprecipitated (IP) with rabbit anti-Chk1 or anti-p-S345 antibodies followed by immunoblotting with mouse anti-Chk1 antibodies. (*B*) Overexpression of wild-type (WT) but not kinase-deficient (KD) Atr enhances S345 phosphorylation of cotransfected Chk1. Thirty-six hours after cotransfection of *CMV:Chk1* and *CMV:FLAG-Atr-WT* or *CMV-FLAG-Atr-KD*, 293T cells were untreated (-) or treated with UV (50 J/m^2) and harvested after 1.5 hr. Whole cell lysates were immunoblotted with anti-FLAG antibodies to detect Atr expression, or assayed for S345 phosphorylation of Chk1 by IP–Western blot as described in (*A*). (*C*) Induction of kinase-deficient Atr inhibits S345 phosphorylation of endogenous Chk1. GM847/ATR-KD cells were cultured in the absence (-) or presence (+) of 1 μg/ml doxycycline (Dox) for 48 hr, untreated (-) or treated with UV (50 J/m^2) and harvested after 1 (1h) or 4 (4h) hr. Whole cell lysates were immunoblotted with anti-FLAG or mouse anti-Chk1 antibodies to detect Atr-KD or endogenous Chk1 expression. And IP–Western was performed to detect S345 phosphorylation of Chk1 as described in *A*.

Discussion

Chk1 is essential for embryonic development and ES cell survival

CHK1 deficiency leads to cell death in ES cells and periimplantation embryonic lethality in mice. Thus, the early lethality of *CHK1* null embryos can be explained by a cell autonomous failure of $CHK1^{-/-}$ embryonic cells to survive. Given the essential role of Chk1 in each cell cycle, it is surprising that *CHK1* null embryos can survive even to the blastocyst stage. A few embryonic divisions may be sustained in the *CHK1* null embryos by maternal Chk1 protein stores. Alternatively, $CHK1^{-/-}$ embryonic cells may be capable of dividing a few times before apoptotic death. Regulated apoptosis occurs in wild-type murine blastocysts and is thought to eliminate redundant or damaged cells before implantation to ensure successful embryonic development (Parchment 1991). Thus, the massive apoptosis displayed by *CHK1* null blastocysts may indicate that $CHK1^{-/-}$ cells accumulate substantial genomic instability. The fact that apoptosis occurs independent of p53 in wild-type and *CHK1* mutant blastocysts is consistent with the previous finding that ES cells undergo p53-independent apoptosis in response to DNA damage (Aladjem et al. 1998).

Although required for DNA damage checkpoints, *CHK1* is not an essential gene in yeast *S. cerevisiae* or *S. pombe*. In contrast, Grapes/Chk1 is indispensable for early embryonic development in fruit flies and, as shown here, in mice. It remains unclear whether this embryonic lethality is due to the cell cycle checkpoint function of Chk1, or to some novel function acquired in evolution. It is known, however, that embryonic development is extremely sensitive to genomic instability. Consistently, disruption of many genes involved in double-stranded DNA break repair, including BRCA1, BRCA2, RAD50, RAD51, and MRE11, lead to early embryonic lethality in mice. Many of these genes have also been shown to be essential for ES cell viability and chromosomal stability (Hakem et al. 1996; Lim and Hasty 1996; Sharan et al. 1997; Luo et al. 1999; Yamaguchi-Iwai et al. 1999). Thus, if Chk1 mutant cells are checkpoint defective and cannot fully repair DNA damage during normal cell cycle, it might lead to the accumulation of genomic instability, cell death, and embryonic lethality.

CHK1 *and* ATR *may define a new class of tumor suppressors*

Given the degree of genomic instability seen in $ATR^{-/-}$ cells and possibly $CHK1^{-/-}$ cells, *CHK1* and *ATR* are likely to be potent tumor suppressor genes. *ATR* heterozygotes have a small increase in tumor incidence (Brown and Baltimore 2000), whereas *CHK1* heterozygosity modestly enhances the tumorgenicity of *WNT-1* oncogenic mice. A limited analysis failed to detect any incidence of loss of heterozygosity (LOH) in $ATR^{+/-}$ or $CHK1^{+/-}$ tumors. This is consistent with the fact that complete absence of these proteins leads to cell lethality. Likewise, increase in spontaneous or carcinogen-induced tumor formation has been observed in p27 heterozygotes and some p53 heterozygotes without LOH (Fero et al. 1998; Venkatachalam et al. 1998). Because *ATR* and *CHK1* are both essential genes that in the heterozygous state can modestly enhance tumorigenesis, they may represent a novel class of essential tumor suppressor genes that fail to display LOH in developing tumors. This also suggests that not all tumor suppressor genes can be detected by simply searching for mutations in the remaining allele of genes within a particular region of LOH. Thus, it might be prudent to give careful consideration to those genes believed to be essential for viability as important candidates for tumor suppressor genes.

Chk1 is required for initiating G_2 arrest after γ-irradiation

In response to IR, mouse ES cells arrest predominantly at G_2 and Chk2 is required to maintain this arrest (Hirao et al. 2000). Similarily, p53, p21, and 14-3-3 sigma have been shown to help sustain the IR-induced G_2 arrest in human fibroblast cells (Bunz et al. 1998; Chan et al. 1999). Our analysis of the conditional *CHK1*-deficient ES cells indicates that Chk1 is primarily responsible for the initiation of G_2 arrest in response to DNA damage. Chk1 and Chk2 have been shown to phosphorylate human Cdc25C on S216 in vitro (Furnari et al. 1997; Sanchez et al. 1997; Matsuoka et al. 1998; Blasina et al. 1999; Brown et al. 1999; Chaturvedi et al. 1999). S216 phosphorylation of Cdc25C is important for G_2 arrest after DNA damage (Peng et al. 1997) because it causes inhibition and cytoplasmic sequestration of Cdc25C, thereby preventing the activation of Cdc2 kinase (Kumagai and Dunphy 1999; Lopez-Girona et al. 1999; Yang et al. 1999). Because the S216 site is not conserved in mouse Cdc25C, other similarly acting phosphorylation sites may exist as targets of these checkpoint kinases. Furthermore, it is likely that additional targets for Chk1 and Chk2 also contribute to cell cycle arrest (O'Connell et al. 1997). Our results are consistent with the model in which Chk1 primarily functions to initiate the G_2 arrest in response to DNA damage and Chk2 plays a supporting role in maintaining this arrest both by preventing the activation of Cdc2 kinase through Cdc25C. Because mouse ES cells have an unusual cell cycle, it will be important to study Chk1 and Chk2 function in DNA damage checkpoints in other cell types.

Chk1 is modified in response to DNA damage

In yeast and humans, Chk1 is phosphorylated in response to DNA damage (Walworth et al. 1993; Sanchez et al. 1997, 1999). The phosphorylation of human Chk1 can only be reliably detected by two-dimensional gel analysis. To establish a simpler assay for Chk1 activation, we made phospho-specific antibodies and found that anti-p-S345 antibodies were able to immunoprecipitate Chk1 efficiently only when cells were treated with DNA-damaging or replication-interfering agents such as UV and HU, and to a lesser extent with IR. Analysis of

Chk1 phosphorylation was complicated by the fact that it runs on a gel at a position obscured by the heavy chain of IgG. The assay we used could not distinguish regulated phosphorylation of Chk1 on S345 versus constitutive phosphorylation with regulated accessibility by antibodies. However, given the knowledge of Chk1 phosphorylation in other systems, we favor the idea that human Chk1 is phosphorylated on S345 in response to DNA damage or replication blocks. The S345 site ISF(pS)QP is very similar to the consensus 14-3-3 binding sequence RSx(pS)xP, suggesting that phosphorylated human Chk1 protein may interact with 14-3-3 proteins. Phosphorylation of this conserved site in *S. pombe* Chk1 could potentially explain the increase in 14-3-3 binding to Chk1 after DNA damage (Chen et al. 1999).

Atr regulates Chk1

Both Atr/Mei-41 and Chk1/Grapes are required for early embryogenesis in mice and fruit flies, suggesting Atr and Chk1 function in the same pathway. We propose that Atr is a major regulator of Chk1 in response to DNA damage based on the following observations: (1) Chk1 phosphorylation on S345 is increased in response to UV and HU treatment, to which cells expressing kinase-defective mutant Atr show enhanced sensitivity (Cliby et al. 1998); (2) overexpression of Atr enhances Chk1 S345 phosphorylation in response to UV; (3) Atr can phosphorylate the S345 site in vitro when presented as a GST fusion peptide (Kim et al. 1999); (4) overexpression of the kinase-defective mutant Atr reduces S345 phosphorylation of endogenous Chk1 in response to UV; and (5) like *CHK1*$^{-/-}$ cells, cells expressing the kinase-defective mutant Atr are compromised for the IR-induced G_2 arrest (Cliby et al. 1998). Taken together, these results suggest that Atr functions upstream of Chk1 and regulate its phosphorylation on S345 in response to DNA damage.

Our results are consistent with a model shown in Figure 7, in which Atm–Chk2 and Atr–Chk1 represent two parallel branches in the mammalian DNA damage response pathway that respond primarily toward different types of DNA damage. Atm responds primarily to DNA-damaging agents that cause double-stranded breaks, such as IR, and phosphorylates Chk2. Atm and Chk2 together phosphorylate Brca1 and p53 (Banin et al. 1998; Canman et al. 1998; Cortez et al. 1999; Chehab et al. 2000; Hirao et al. 2000; Shieh et al. 2000), and activate cellular responses including G_1 arrest. On the other hand, Atr responds primarily to agents like UV and HU that can potentially interfere with DNA replication, and phosphorylates Chk1. It is possible that Atr and Chk1 phosphorylate Brca1, p53 in addition to Cdc25C (Tibbetts et al. 1999; Shieh et al. 2000; R.S. Tibbetts et al., in prep.), and activate cellular responses including G_2 arrest. Furthermore, the two pathways have significant overlap and often cooperate with each other to ensure prompt and efficient repair of DNA damage and to maintain genomic integrity. When one pathway is genetically compromised, they can also function redundantly, although probably to a lesser extent and with different kinetics. For example, the rapid p53 stabilization in response to IR is greatly reduced in *ATM* mutant cells (Kastan et al. 1992), but it does occur much later, which is probably due to Atr (Lu and Lane 1993; Tibbetts et al. 1999). Similar observations have been made for Chk2 phosphorylation in response to IR (S. Matsuoka and S.J. Elledge, unpubl.). This may reflect the fact that in addition to tailoring the cellular response to different types of DNA damage, cells have many responses that are commonly required toward different types of genotoxic stress.

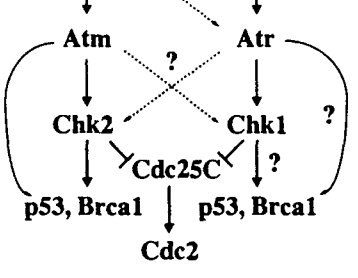

Figure 7. A model for the mammalian DNA damage response pathway (See text for details). The question marks indicate hypothetical regulatory interactions.

Materials and methods

Construction of targeting vectors

All targeting vectors were constructed for positive–negative selection and thus contain a *neo* or *hprt* marker and a *TK* marker. For simplification, we describe the composition of each vector rather than details of construction. *Neo*-targeting vector (pQL258): The *neo* marker was flanked by 1.9 kb of the 5′ untranslated region and 4.5 kb of genomic sequence containing exons 6–7. Hprt-targeting vector (pQL289): The *hprt* marker was flanked by 3 kb of 5′ genomic sequence with exon 2 and 4.2 kb of 3′ genomic sequence with exons 6–7. Flox targeting vector (pQL456): The *lox*P–*neo*–*lox*P cassette was ligated to a 2.2-kb exon 2-containing genomic sequence, of which the last 59 bp was replaced by an *Eco*RV and a *lox*P site. The *lox*P–*neo*–*lox*P–E2–*Rv*–*lox*P centerpiece was flanked by 1.9 kb of 5′ untranslated region and 4.3 kb of 3′ genomic sequence carrying exons 3–5.

Southern blot and PCR

Genomic DNA was isolated from ES cells or mouse tissues using standard protocols and Southern blot analysis were performed with QuikHyb solution (Stratagene). The 3′ external probe was a 420-bp *Hin*dIII–*Nhe*I fragment from pQL253, whereas the 5′ internal probe was a 1.4-kb *Eco*RI–*Xho*I fragment from pQL286. *WNT-1* and p53 genotyping was performed as described (Tsukamoto et al. 1988; Donehower et al. 1992). Preimplantation embryos were digested at 55°C overnight in lysis buffer [10 mM Tris (pH 7.5), 10 mM EDTA (pH 8), 10 mM NaCl, 0.5% Sarcosyl, 0.5 mg/ml protease K] and 1–5 µl lysate was used for PCR. *CHK1* PCR was conducted in 25 µl reaction using Expand DNA polymerase (Boehringer Mannheim) and three primers: 247, 5′-ACCGCTTCCTCGTGCTTTAC-3′; 248, 5′-ATAGGCACCTTCTCCCAAAG-3′; and 252, 5′-GGAGGA-

CAAACGTGGAAACAGG-3′. PCR cycles: 94°C, 3 min, 33 cycles of (94°C, 20 sec; 63°C, 60 sec), 68°C, 4 min. A 282-bp and a 572-bp fragment were amplified from the wild type (by 248 and 252) and mutant alleles (by 247 and 252), respectively.

Manipulations of pre-implantation embryos

All embryos were generated by natural matings. Eight-cell morula were cultured in KSOM media (Cell and Molecular Technologies) and blastocysts in M15 media. All images of in vitro cultured embryos were taken on an inverted microscope using the National Institutes of Health (NIH) imaging software.

TUNEL analysis of blastocysts

Eight-cell morula were isolated, cultured for 45 hr and harvested for TUNEL analysis according to manufacture's protocol (Boehringer Mannheim). In brief, embryos were fixed in 10% formalin for 20 min, permeablized in 0.2% Triton X-100 for 5 min, followed by TUNEL labeling at 37°C for 1 hr and DAPI staining. Stained embryos were individually suspended in PBS solution for imaging on a Zeiss fluorescence microscope. Mutant and normal-looking embryos were divided into two groups: half for genotyping and half mounted for confocal imaging. Normal (*CHK1*$^{+/+}$ and *CHK1*$^{+/-}$) versus mutant (*CHK1*$^{-/-}$) embryos were identified with ~95% confidence.

FACS and mitotic index

FACS analysis was performed with standard protocols. Feeder cells were excluded based on their giant size and greater than 4N DNA content. The percentage of G_1–S and G_2 population was measured by the Coulter (II) software (Beckman). For mitotic index measurement, cells were cytospinned onto slides, fixed in 3% paraformaldehyde for 15 min, permeablized in 0.5% NP40 for 5 min, and mounted in Vectashield containing DAPI (Vector Lab). Feeder cells were excluded based on their giant size and multinuclei.

Antibodies

Mouse anti-FLAG (M5) (Sigma) and anti-Chk1 (Santa Cruz) antibodies were purchased and rabbit anti-(human) Chk1 antibodies were described in Sanchez et al. (1997). The anti-p-S345 antibodies were raised against a human Chk1 phospho-S345 peptide, QGISF(pS)QPTC, and were affinity-purified by the phospho–antigen-peptide column followed by passing through a QGISFSQPTC peptide column to eliminate nonspecific antibodies reacting with the unphosphorylated antigen peptide. Cell lysates were prepared and immunoprecipitation (IP) were performed as described (Matsuoka et al. 1998). IP with anti-p-S345 antibodies was conducted in the presence of 100 μg/ml of the QGISFSQPTC peptide. Immunoblots were visualized by ECL (Amersham).

Acknowledgments

We thank Drs. Yolonda Sanchez, Stephen H. Friend, Karlene A. Cimprich, Philippe Soriano, and Richard Behringer for useful plasmids and reagents, Janet C. Thompson, Louise A. Stanley, and Jessica Wang for technical assistance. We also thank Dr. Michael A. Mancini for generous help on confocal imaging, Drs. Pauline Ward and Zhengzheng Shi for technical advice on manipulation of preimplantation embryos, and Hua Chang, Drs. Tony Carr, Nancy Walworth, Eric Brown, William Sullivan, Anthony Lau, and Pumin Zhang for helpful discussions. X.C. is supported by Karolinska Institute (Sweden)/BCM exchange program and the U.S. Army Breast Cancer Research program. L.A.D. is the recipient of a U.S. Army Breast Cancer Research Program academic award. This work was also supported by NIH grants awarded to S.J.E. and A.B. Both are investigators with the Howard Hughes Medical Institute.

The publication costs of this article were defrayed in part by payment of page charges. This article must therefore be hereby marked "advertisement" in accordance with 18 USC section 1734 solely to indicate this fact.

References

Aladjem, M.I., B.T. Spike, L.W. Rodewald, T.J. Hope, M. Klemm, R. Jaenisch, and G.M. Wahl. 1998. ES cells do not activate p53-dependent stress responses and undergo p53-independent apoptosis in response to DNA damage. *Curr. Biol.* **8:** 145–155.

Al-Khodairy, F., E. Fotou, K.S. Sheldrick, D.J. Griffiths, A.R. Lehmann, and A.M. Carr. 1994. Identification and characterization of new elements involved in checkpoint and feedback controls in fission yeast. *Mol. Biol. Cell.* **5:** 147–160.

Banin, S., L. Moyal, S. Shieh, Y. Taya, C.W. Anderson, L. Chessa, N.I. Smorodinsky, C. Prives, Y. Reiss, Y. Shiloh et al. 1998. Enhanced phosphorylation of p53 by ATM in response to DNA damage. *Science* **281:** 1674–1677.

Barlow, C., S. Hirotsune, R. Paylor, M. Liyanage, M. Eckhaus, F. Collins, Y. Shiloh, J.N. Crawley, T. Ried, D. Tagle et al. 1996. Atm-deficient mice: A paradigm of ataxia telangiectasia. *Cell* **86:** 159–171.

Blasina, A., D. Weyer IV, M.C. Laus, W.H. Luyten, A.E. Parker, and C.H. McGowan. 1999. A human homologue of the checkpoint kinase Cds1 directly inhibits Cdc25 phosphatase. *Curr. Biol.* **9:** 1–10.

Boddy, M.N., B. Furnari, O. Mondesert, and P. Russell. 1998. Replication checkpoint enforced by kinases Cds1 and Chk1. *Science* **280:** 909–912.

Brown, A.L., C.H. Lee, J.K. Schwarz, N. Mitiku, H. Piwnica-Worms, and J.H. Chung. 1999. A human Cds1-related kinase that functions downstream of ATM protein in the cellular response to DNA damage. *Proc. Natl. Acad. Sci.* **96:** 3745–3750.

Brown, E.J. and D. Baltimore. 2000. ATR disruption leads to chromosomal fragmentation and early embryonic lethality. *Genes & Dev.* **14:** 397–402.

Bunz, F., A. Dutriaux, C. Lengauer, T. Waldman, S. Zhou, J.P. Brown, J.M. Sedivy, K.W. Kinzler, and B. Vogelstein. 1998. Requirement for p53 and p21 to sustain G2 arrest after DNA damage. *Science* **282:** 1497–1501.

Canman, C.E., D.S. Lim, K.A. Cimprich, Y. Taya, K. Tamai, K. Sakaguchi, E. Appella, M. B. Kastan, and J.D. Siliciano. 1998. Activation of the ATM kinase by ionizing radiation and phosphorylation of p53. *Science* **281:** 1677–1679.

Chan, T.A., H. Hermeking, C. Lengauer, K.W. Kinzler, and B. Vogelstein. 1999. 14-3-3Sigma is required to prevent mitotic catastrophe after DNA damage. *Nature* **401:** 616–620.

Chaturvedi, P., W.K. Eng, Y. Zhu, M.R. Mattern, R. Mishra, M.R. Hurle, X. Zhang, R.S. Annan, Q. Lu, L.F. Faucette et al. 1999. Mammalian Chk2 is a downstream effector of the ATM-dependent DNA damage checkpoint pathway. *Oncogene* **18:** 4047–4054.

Chehab, N.H., A. Malikzay, M. Appel, and T.D. Halazonetis. 2000. Chk2/hCds1 functions as a DNA damage checkpoint in G(1) by stabilizing p53. *Genes & Dev.* **14:** 278–288.

Chen, L., T.H. Liu, and N.C. Walworth. 1999. Association of Chk1 with 14-3-3 proteins is stimulated by DNA damage. *Genes & Dev.* **13:** 675–685.

Cimprich, K.A., T.B. Shin, C.T. Keith, and S.L. Schreiber. 1996. cDNA cloning and gene mapping of a candidate human cell cycle checkpoint protein. *Proc. Natl. Acad. Sci.* **93:** 2850–2855.

Cliby, W.A., C.J. Roberts, K.A. Cimprich, C.M. Stringer, J.R. Lamb, S.L. Schreiber, and S.H. Friend. 1998. Overexpression of a kinase-inactive ATR protein causes sensitivity to DNA-damaging agents and defects in cell cycle checkpoints. *EMBO J.* **17:** 159–169.

Cortez, D., Y. Wang, J. Qin, and S.J. Elledge. 1999. Requirement of ATM-dependent phosphorylation of Brca1 in the DNA damage response to double-strand breaks. *Science* **286:** 1162–1166.

Donehower, L.A., M. Harvey, B.L. Slagle, M.J. McArthur, C.A. Montgonery Jr., J.S. Butel, and A. Bradley. 1992. Mice deficient for p53 are developmentally normal but susceptible to spontaneous tumors. *Nature* **356:** 215–221.

Donehower, L.A., L.A. Godley, C.M. Aldaz, R. Pyle, Y.P. Shi, D. Pinkel, J. Gray, A. Bradley, D. Medina, and H.E. Varmus. 1995. Deficiency of p53 accelerates mammary tumorigenesis in Wnt-1 transgenic mice and promotes chromosomal instability. *Genes & Dev.* **9:** 882–895.

Elledge, S.J. 1996. Cell cycle checkpoints: Preventing an identity crisis. *Science* **274:** 1664–1672.

Fero, M.L., E. Randel, K.E. Gurley, J.M. Roberts, and C.J. Kemp. 1998. The murine gene p27Kip1 is haplo-insufficient for tumour suppression. *Nature* **396:** 177–180.

Fogarty, P., S.D. Campbell, R. Abu-Shumays, B.S. Phalle, K.R. Yu, G.L. Uy, M.L. Goldberg, and W. Sullivan. 1997. The Drosophila grapes gene is related to checkpoint gene chk1/rad27 and is required for late syncytial division fidelity. *Curr. Biol.* **7:** 418–426.

Furnari, B., N. Rhind, and P. Russell. 1997. Cdc25 mitotic inducer targeted by chk1 DNA damage checkpoint kinase. *Science* **277:** 1495–1497.

Hakem, R., J.L. de la Pompa, C. Sirard, R. Mo, M. Woo, A. Hakem, A. Wakeham, J. Potter, A. Reitmair, F. Billia et al. 1996. The tumor suppressor gene Brca1 is required for embryonic cellular proliferation in the mouse. *Cell* **85:** 1009–1023.

Hirao A., Y. Kong, S. Matsuoka, A. Wakeham, J. Ruland, H. Yoshida, D. Liu, S.J. Elledge, and T.W. Mak. 2000. DNA damage-induced activation of p53 by the checkpoint kinase Chk2. *Science* **287:** 1824–1827.

Jones, J.M., X.-S. Cui, D. Medina, and L.A. Donehower. 1999. Heterozygosity of p21 WAF1/CIP1 enhances tumor cell proliferation and cyclin D1-associated kinase activity in a murine mammary cancer model. *Cell Growth Differ.* **10:** 213–222.

Kastan, M.B., Q. Zhan, W.S. el-Deiry, F. Carrier, T. Jacks, W.V. Walsh, B.S. Plunkett, B. Vogelstein, and A.J. Fornace. 1992. A mammalian cell cycle checkpoint pathway utilizing p53 and GADD45 is defective in ataxia-telangiectasia. *Cell* **71:** 587–597.

Keegan, K.S., D.A. Holtzman, A.W. Plug, E.R. Christenson, E.E. Brainerd, G. Flaggs, N.J. Bentley, E.M. Taylor, M.S. Meyn, S.B. Moss et al. 1996. The Atr and Atm protein kinases associate with different sites along meiotically pairing chromosomes. *Genes & Dev.* **10:** 2423–2437.

Kim, S.T., D.S. Lim, C.E. Canman, and M.B. Kastan. 1999. Substrate specificities and identification of putative substrates of ATM kinase family members. *J. Biol. Chem.* **274:** 37538–37543.

Kumagai, A. and W.G. Dunphy. 1999. Binding of 14-3-3 proteins and nuclear export control the intracellular localization of the mitotic inducer Cdc25. *Genes & Dev.* **13:** 1067–1072.

Kumagai A., Z. Guo, K.H. Emami, S.X. Wang, and W.G. Dunphy. 1998. The Xenopus Chk1 protein kinase mediates a caffeine-sensitive pathway of checkpoint control in cell-free extracts. *J. Cell. Biol.* **142:** 1559–1569.

Lim, D.S. and P. Hasty. 1996. A mutation in mouse rad51 results in an early embryonic lethal that is suppressed by a mutation in p53. *Mol. Cell. Biol.* **16:** 7133–7143.

Lindsay, H.D., D.J. Griffiths, R.J. Edwards, P.U. Christensen, J.M. Murray, F. Osman, N. Walworth, and A.M. Carr. 1998. S-phase-specific activation of Cds1 kinase defines a subpathway of the checkpoint response in *Schizosaccharomyces pombe*. *Genes & Dev.* **12:** 382–395.

Lopez-Girona, A., B. Furnari, O. Mondesert, and P. Russell. 1999. Nuclear localization of Cdc25 is regulated by DNA damage and a 14-3-3 protein. *Nature* **397:** 172–175.

Lu, X. and D.P. Lane. 1993. Differential induction of transcriptionally active p53 following UV or ionizing radiation: Defects in chromosome instability syndromes? *Cell* **75:** 765–778.

Luo, G., M.S. Yao, C.F. Bender, M. Mills, A.R. Bladl, A. Bradley, and J.H. Petrini. 1999. Disruption of mRad50 causes embryonic stem cell lethality, abnormal embryonic development, and sensitivity to ionizing radiation. *Proc. Natl. Acad. Sci.* **96:** 7376–7381.

Matsuoka, S., M. Huang, and S.J. Elledge. 1998. Linkage of ATM to cell cycle regulation by the Chk2 protein kinase. *Science* **282:** 1893–1897.

Nakajo, N., T. Oe, K. Uto, and N. Sagata. 1999. Involvement of Chk1 kinase in prophase I arrest of Xenopus oocytes. *Dev. Biol.* **207:** 432–444.

O'Connell, M.J., J.M. Raleigh, H.M. Verkade, and P. Nurse. 1997. Chk1 is a wee1 kinase in the G2 DNA damage checkpoint inhibiting cdc2 by Y15 phosphorylation. *EMBO J.* **16:** 545–554.

Parchment, R.E. 1991. Programmed cell death (apoptosis) in murine blastocysts: Extracellular free-radicals, polyamines, and other cytotoxic agents. *In Vivo* **5:** 493–500.

Peng, C-Y., P.R. Graves, R.S. Thoma, Z. Wu, A.S. Shaw, and H. Piwnica-Worms. 1997. Mitotic and G2 checkpoint control: Regulation of 14-3-3 protein binding by phosphorylation of Cdc25C on serine-216. *Science* **277:** 1501–1505.

Sanchez, Y., B.A. Desany, W.J. Jones, Q, Liu, B. Wang, and S.J. Elledge. 1996. Regulation of RAD53 by the ATM-like kinases MEC1 and TEL1 in yeast Cell Cycle Checkpoint Pathways. *Science* **271:** 357–360.

Sanchez, Y., C. Wong, R.S. Thoma, R. Richman, Z. Wu, H. Piwnica-Worms, and S.J. Elledge. 1997. Conservation of the Chk1 checkpoint pathway in mammals: Linkage DNA damage to Cdk regulation through Cdc25. *Science* **277:** 1497–1501.

Sanchez, Y., J. Bachant, H. Wang, F. Hu, D. Liu, M. Tetzlaff, and S.J. Elledge. 1999. Control of the DNA damage checkpoint by chk1 and rad53 protein kinases through distinct mechanisms. *Science* **286:** 1166–1171.

Savitsky, K., A. Bar-Shira, S. Gilad, G. Rotman, Y. Ziv, L. Vanagaite, D.A. Tagle, S. Smith, T. Uziel, S. Sfez et al. 1995. A single ataxia telangiectasia gene with a product similar to PI-3 kinase. *Science* **268:** 1749–1753.

Sharan, S.K., M. Morimatsu, U. Albrecht, D.S. Lim, E. Regel, C. Dinh, A. Sands, G. Eichele, P. Hasty, and A. Bradley. 1997. Embryonic lethality and radiation hypersensitivity mediated by Rad51 in mice lacking Brca2. *Nature* **386:** 804–810.

Shieh, S.Y., J. Ahn, K. Tamai, Y. Taya, and C. Prives. 2000. The human homologs of checkpoint kinases chk1 and cds1

(Chk2) phosphorylate p53 at multiple DNA damage-inducible sites. *Genes & Dev.* **14:** 289–300.

Sibon, O.C., V.A. Stevenson, and W.E. Theurkauf. 1997. DNA-replication checkpoint control at the Drosophila midblastula transition. *Nature* **388:** 93–97.

Sibon, O.C., A. Laurencon, R. Hawley, and W.E. Theurkauf. 1999. The Drosophila ATM homologue Mei-41 has an essential checkpoint function at the midblastula transition. *Curr. Biol.* **9:** 302–312.

Su, T.T., S.D. Campbell, and P.H. O'Farrell. 1999. Drosophila grapes/CHK1 mutants are defective in cyclin proteolysis and coordination of mitotic events. *Curr. Biol.* **9:** 919–922.

Sun, Z., D.S. Fay, F. Marini, M. Foiani, and D.F. Stern. 1996. Spk1/Rad53 is regulated by Mec1-dependent protein phosphorylation in DNA replication and damage checkpoint pathways. *Genes & Dev.* **10:** 395–406.

Tibbetts, R.S., K.M. Brumbaugh, J.M. Williams, J.N. Sarkaria, W.A. Cliby, S.Y. Shieh, Y. Taya, C. Prives, and R.T. Abraham. 1999. A role for ATR in the DNA damage-induced phosphorylation of p53. *Genes & Dev.* **13:** 152–157.

Tsukamoto, A.S., R. Grosschedl, R.C. Guman, T. Parslow, and H.E. Varmus. 1988. Expression of the *int-1* gene in transgenic mice is associated with mammary gland hyperplasia and adenocarcinomas in male and female mice. *Cell* **55:** 619–625.

Venkatachalam, S., Y.P. Shi, S.N. Jones, H. Vogel, A. Bradley, D. Pinkel, and L.A. Donehower. 1998. Retention of wild-type p53 in tumors from p53 heterozygous mice: Reduction of p53 dosage can promote cancer formation. *EMBO J.* **17:** 4657–4667.

Walworth, N.C. and R. Bernards. 1996. Rad-dependent response of the chk1-encoded protein kinase at the DNA damage checkpoint. *Science* **271:** 353–356.

Walworth, N., S. Davey, and D. Beach. 1993. Fission yeast chk1 protein kinase links the rad checkpoint pathway to cdc2. *Nature* **363:** 368–371.

Wright, J.A., K.S. Keegan, D.R. Herendeen, N.J. Bentley, A.M. Carr, M.F. Hoekstra, and P. Concannon. 1998. Protein kinase mutants of human ATR increase sensitivity to UV and ionizing radiation and abrogate cell cycle checkpoint control. *Proc. Natl. Acad. Sci.* **95:** 7445–7450.

Xu, Y., T. Ashley, E.E. Brainerd, R.T. Bronson, M.S. Meyn, and D. Baltimore. 1996. Targeted disruption of ATM leads to growth retardation, chromosomal fragmentation during meiosis, immune defects, and thymic lymphoma. *Genes & Dev.* **10:** 2411–2422.

Yamaguchi-Iwai, Y., E. Sonoda, M.S. Sasaki, C. Morrison, T. Haraguchi, Y. Hiraoka, Y.M. Yamashita, T. Yagi, M. Takata, C. Price et al. 1999. Mre11 is essential for the maintenance of chromosomal DNA in vertebrate cells. *EMBO J.* **18:** 6619–6629.

Yang, J., K. Winkler, M. Yoshida, and S. Kornbluth. 1999. Maintenance of G2 arrest in the Xenopus oocyte: A role for 14-3-3-mediated inhibition of Cdc25 nuclear import. *EMBO J.* **18:** 2174–2183.

Vol. 11, 0000–0000, July 2000

p190-B, a Rho-GTPase-activating Protein, Is Differentially Expressed in Terminal End Buds and Breast Cancer[1]

Geetika Chakravarty, Deana Roy, Maria Gonzales, Jason Gay, Alejandro Contreras, and Jeffrey M. Rosen[2]

Department of Cell Biology, Baylor College of Medicine, Houston, Texas 77030

Abstract

Microdissection and differential display PCR were used to identify genes preferentially expressed in the highly proliferative terminal end buds (TEBs) in the mammary gland of 45-day-old virgin rats. One clone exhibited 87% homology to the human *p190-B* gene encoding a novel Rho-Gap. Using *in situ* hybridization, p190-B was detected in both the TEBs and the terminal ducts, with the highest expression observed in the outer layer of TEBs. During normal mammary gland development, p190-B mRNA expression was highest in the virgin mammary gland and decreased during late pregnancy and lactation. Interestingly, increased levels of p190-B mRNA relative to the normal mammary gland were seen in a subset of murine mammary tumors that appeared to be less well differentiated and potentially more aggressive. Transient transfection of a p190-B expression construct into MCF-10A human mammary epithelial cells resulted in disruption of the actin cytoskeleton, which suggests a role for p190-B in regulating the signaling pathways that influence cell migration and invasion. These results suggest that p190-B may be required for virgin mammary gland development, and its aberrant expression may occur in breast cancer.

Introduction

A woman's reproductive history is one of the principal determinants of her susceptibility to breast cancer. An early full-term pregnancy is protective and the length of time between menarche and the first full-term pregnancy seems to be critical for the initiation of breast cancer (1). This phenomenon has been extensively modeled in rat model systems, in which pregnancy *per se* (2), (3) or treatment with estrogen and progesterone has been shown to be highly protective against NMU[3]-induced carcinogenesis (4, 5). Recently, parity-induced protection has also been reproduced in a mouse model (6). Although the mechanism for this protective effect has not been defined, Russo and Russo (7) have suggested that the protective effects of an early full-term pregnancy result from estrogen- and progesterone-induced differentiation of mammary epithelial cells and the concomitant loss of cells susceptible to carcinogenesis. The effects of estrogen and progesterone are mediated by the induction of specific "local mediators," *i. e.*, growth factors that act via autocrine and paracrine mechanisms to influence TD and TEB growth and differentiation (8). These factors may induce persistent alterations in intracellular pathways that govern the proliferative response of mammary cells to carcinogenic action (9). An alternative to Russo's hypothesis suggests, however, that other alterations in addition to differentiation of the TEB and TD might explain the refractoriness to mammary carcinogenesis (10). Regardless of which hypothesis is correct, no molecular markers are available to identify and follow the fate of the highly susceptible TEB cells. Yet, such intermediate biomarkers will be required to develop effective diagnostic tools and preventive therapies for breast cancer.

TEBs are composed of highly proliferative cells thought to be the most susceptible to neoplastic transformation. Ductal morphogenesis is accompanied by the penetration of these proliferative cells into the surrounding fat pad. The TEB contains two histologically distinct cell types: the more central body cells and the outer cap cells. The highest levels of proliferation are observed in the cap cells, whereas the body cells surrounding the lumen are highly apoptotic, thus providing a mechanism to generate a ductal structure (11). With each estrous cycle, most of the TEBs in mature animals progressively differentiate into ABS. A small population become atrophic and give rise to TDs. Both TEBs and TDs are targets for carcinogen action in young and old virgin rats, respectively.

The objective of this study was to identify molecular markers for TEB and TD cells to follow their fate during mammary development and carcinogenesis. To do so, we sought to identify genes that were differentially expressed between TEBs and the M and S regions of the nulliparous rat mammary gland. A large repertoire of techniques, such as subtractive hybridization of cDNA (12), cDNA arrays (13), representational difference analysis (14), and SAGE (reviewed in Ref. 15), now exist that are capable of generating a profile

Received 6/21/99; revised 3/15/00; accepted 5/22/00.
The costs of publication of this article were defrayed in part by the payment of page charges. This article must therefore be hereby marked *advertisement* in accordance with 18 U.S.C. Section 1734 solely to indicate this fact.
[1] This work was supported by grants from the Army Breast Cancer Research Program USAMRDC DAMD 17-94-J4253 and by NIH Grant CA64255.
[2] To whom requests for reprints should be addressed, at Department of Cell Biology, Baylor College of Medicine, Houston, TX 77030. E-mail: jrosen@bcm.tmc.edu.

[3] The abbreviations used are: NMU, nitrosomethylurea; TD, terminal duct; EB, end bud; TEB, terminal EB; EDD, EB DD; ABS, alveolar buds; DD, differential display; GAPDH, glyceraldehyde-3-phosphate dehydrogenase; K18, Keratin-18; RT, reverse transcription; M, midgland (tissue); S, stroma/stromal (tissue); ECM, extracellular matrix; TRAP, telomeric repeat amplification protocol; DAPI, 4′,6-diamidino-2-phenylindole; EtBr, ethidium bromide; oligo(dT), oligodeoxythymidylic acid;

SAGE, Serial analysis of gene expression; IACUC, Institutional animal care and use

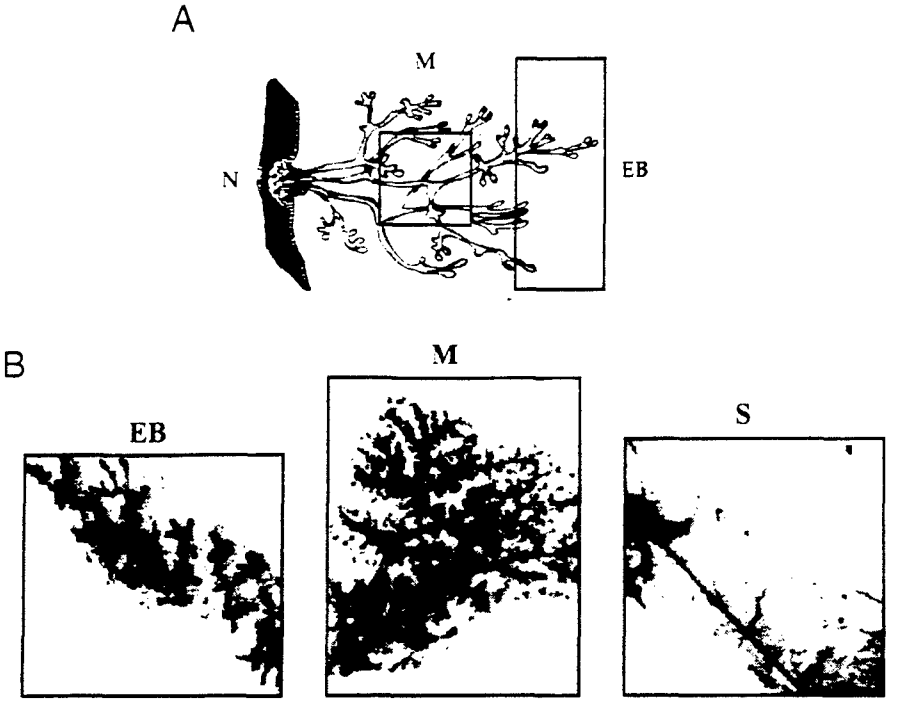

Fig. 1. Isolation of mammary tissue fractions by dye visualization. *A*, diagram of the virgin mammary gland; end bud (*EB*), midgland (*M*), and nipple (*N*), adapted from Ref. 25. *B*, mammary tissue fractions dissected from a 45-day-old nulliparous rat after visualization of the ductal tree with trypan blue; stroma (*S*).

that reflects the presence of differentially expressed transcripts. However, with DD-PCR (16), multiple RNA samples can be compared at one time. Moreover, as little as 5 μg of total RNA per sample is enough to carry out the analysis. Thus, when these studies were initiated, DD-PCR was the preferred method because only microgram quantities of RNA could be isolated from the various dissected regions of the mammary gland. In all, 14 differentially expressed cDNA fragments were subcloned from the TEB region and sequenced to identify potentially interesting genes. This study reports the identification and characterization of a Rho-GTPase-activating protein, p190-B, that may be required for virgin mammary gland development and may play a role in mammary neoplasia.

Results

Isolation of TEB Specific Genes. DD-PCR analysis of the RNA samples obtained from the dissection of TEB and of M and S regions of the rat virgin mammary gland (Fig. 1) resulted in the isolation of 14 clones that were preferentially expressed in the TEB (Fig. 2). Some of these clones were identified because their differential expression pattern could be reproduced in parallel runs of two different pools of RNA (see Fig. 2, *A* and *B*). Homology searches were performed using BLAST (software) searches against the GenBank database (17). A summary of the genes showing homology to the EDD clones is presented in Table 1. Ten of the EDD clones had a high similarity to sequences in the database. Although five of these clones are expressed sequence tags (ESTs) with unknown functions, the remaining clones were identified as genes whose products perform a wide range of actions: growth factor, signaling molecule, cell surface receptor, mitochondrial product, and a mineral binding protein.

To further confirm these results, we followed the expression of EDD clones by "Reverse Northern," in which a fixed amount of each of the amplified DD-PCR clone was run on high-density gels and were probed with reverse-transcribed radiolabeled cRNA probes. Unlike conventional Northern analysis, in this technique, the cDNA clones are blotted onto nylon membranes and probed with reverse-transcribed cRNA probes (12). The abundance of a transcript in the RNA used for RT should determine the signal intensity on the blot. This method was used because of the relatively low abundance and the difficulty in obtaining poly(A)+ RNA from micro-dissected TEB fractions required for Northern blot or RNase protection analyses. To increase the sensitivity of the assay, each of the selected clones was run in duplicate at two different concentrations. Expression of housekeeping genes like *GAPDH* and *L19* were used to monitor the efficiency of RT reaction whereas K18, expressed only in epithelial cells, provided the positive control to determine the sensitivity of this method to identify differentially expressed genes. K18 expression was detected in both TEB and M fractions. which contain primarily epithelial cells, whereas the S fraction, which is exclusively from S, was negative for K18 expression (Fig. 3).

Despite the limitations of microdissecting a three-dimensional structure, Reverse Northern analysis confirmed the overexpression of EDDC2 in the TEB fraction (Fig. 3). Although, Reverse Northern analysis revealed only a minimal increase in C2 expression in TEB fractions, it may still have important functional ramifications inasmuch as all of the

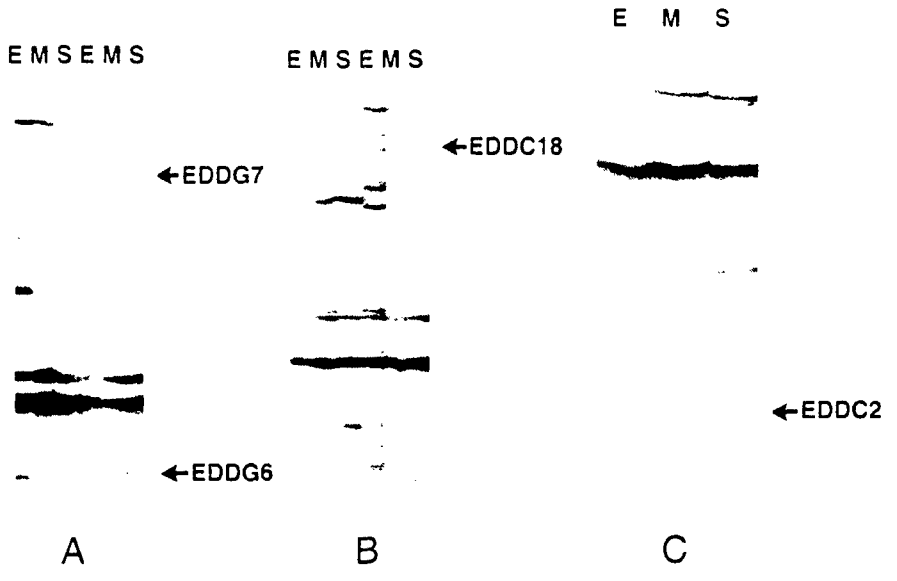

Fig. 2. Representative denaturing polyacrylamide gel for DD analysis to detect cDNAs preferentially expressed in EB fraction of the mammary gland. ^{35}S-labeled dATP DD-PCR products from three sets of RNA designated E, M, and S were run in adjacent lanes. *A*, DD gels using primer combination (T_{11}-G + AP2); *B*, DD gels using primer combination (T_{11}-C + AP8); *C*, DD gels using primer combination (T_{11}-C + AP7). To minimize false-positive bands, each reaction was performed from two independent pools of RNA, and only those bands that were reproducible (*arrows*) were picked up for further analysis. To control for false positives from contaminating DNA, a −RT reaction was subjected to the same PCR conditions and run in parallel lanes (data not shown).

Table 1 Summary chart of genes that are preferentially expressed in TEB region of the rat virgin mammary gland

The DD-PCR clones were compared to GenBank sequences to identify potential homologues using a BLASTN search.

Clone	Primers	Size (bp)	Identity
EDD-G5	AP-7, T11-G	257	LR11 low-density lipoprotein receptor; 90%
EDD-G6	AP-2, T11-G	183	
EDD-G7	AP-2, T11-G	230	
EDD-C2	AP-7, T11-C	241	p190-B Rho GAP; 87%
EDD-C3	AP-7, T11-C	204	yy55h09.s1; cDNA clone 277505; human ovary; 80%
EDD-C6	AP-1, T11-C	122	yf99a06.r1; cDNA clone 30458; human infant brain; 81%
EDD-C11	AP-8, T11-C	92	Calcium binding protein Cab45; 86%
EDD-C12	AP-8, T11-C	108	Adrenomedullin; 100%
EDD-C13	AP-8, T11-C	125	
EDD-C14	AP-8, T11-C	132	yn84b02.s1; cDNA clone 175083; human adult brain; 78%
EDD-C15	AP-8, T11-C	145	yw25b09.s1; cDNA clone 253241; human fetal cochlea; 91%
EDD-C16	AP-8, T11-C	151	Rat mitochondrial rRNA; 98%
EDD-C17	AP-8, T11-C	181	Rat cytochrome C oxidase; 99%
EDD-C18	AP-8, T11-C	422	

DD-PCR clones encoded very low abundance mRNAs when compared with genes like *GAPDH* and *K18*, which were used as positive controls for this experiment. Expression of Clone G7 on the other hand was high in both TEB and S fractions. Similarly, G5 expression was high in S and M fractions. Some of the clones, however, did not provide a significant signal over background and were still below the level of detection by Reverse Northern and, hence, could not be quantitated using the phosphorrimager. Although DD-PCR analysis revealed several-fold higher expression of EDD clones G6, G7, and C18 in TEB fraction (Fig. 2) and looked more promising when compared with EDD clone C2 (see Fig. 2), additional studies were restricted to EDD clone C2 for the following reasons: (*a*) differential expression of this clone could be confirmed by more than one technique; and (*b*) as opposed to G6, G7, and C18, which had no homology to known genes and necessitated isolation of full-length clones, EDD clone C2 was 87% homologous to a novel Rho-Gap family member, p190-B, in a non-Rho-Gap region. A full-length p190-B clone was, thus, available for further analysis to determine whether it was differentially expressed during mammary development and carcinogenesis.

Localization of p190-B Transcripts by *in Situ* Hybridization. p190-B belongs to the Rho-Gap family of proteins and has many family members, the closest being p190-A. p190-B has been implicated in integrin signaling and cytoskeletal reorganization (18). Because p190-Rho-Gaps enhance the conversion of GTP-Rho to GDP-Rho, they negatively regulate cytoskeletal assembly and have a role in cell motility and invasion. (See review 19).

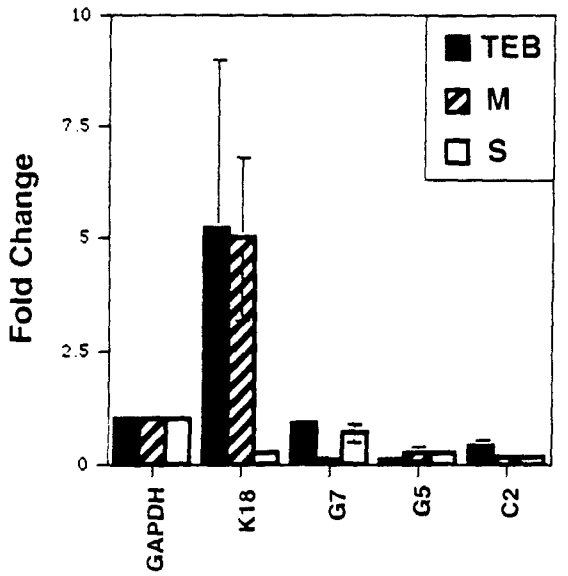

Fig. 3. Quantitative analysis of p190-B expression in TEB, M, and S fractions of the mammary gland by Reverse Northern: DD-PCR clones were PCR-amplified, and an equal of amount of each of the clone was run in duplicate in a three-tier gel system and hybridized with oligo(dT)-primed ^{32}P-radiolabeled reverse-transcribed cDNA (see ~~text~~) from EB, M, and S fractions. The filters were exposed to phosphorimager overnight and quantitated using the software Imagequant (Molecular Dynamics). The data were normalized for RPL19 expression and represent the mean fold-change over GAPDH expression ± SE. Results are representative of three independent experiments.

To confirm the differential tissue distribution of p190-B in the virgin mammary gland, the cDNA was linearized to generate a ^{33}P-riboprobe for the detection of its transcript at the single cell level by *in situ* hybridization. In agreement with the DD-PCR and Reverse Northern data, *in situ* hybridization revealed that the highly proliferative and invasive TEBs displayed the highest expression of p190-B (Fig. 4*A*). Maximum level of p190-B message appears to be in the outer cell layer (Fig. 4*A*, *arrow*). Heterogeneous expression levels of p190-B were also observed in the ABS and ducts and in the S but at much reduced levels (compare the signal seen in TEBs (Fig. 4*A*) with the signal seen in ABS (Fig. 4*D*) and ducts (Fig. 4*G*) over the background as seen in the sense controls depicted in Fig. 4, *C*, *F*, and *I* on serial sections). These results suggest that p190-B may play a role in normal mammary gland development by facilitating the invasion of the TEBs into the surrounding fat pad. Because neither good polyclonal nor good monoclonal antibodies for p190-B were available, these results could not be further confirmed at the protein level using immunohistochemical methods.

p190-B Gene Expression during Mammary Development. In addition to systemic hormones and local growth factors, the S, ECM, and ECM-signaling proteins play a critical role in tissue remodeling and mammary gland development. Because p190-B may be directly involved in the regulation of the actin cytoskeleton and may, therefore, influence mammary morphogenesis, its expression was analyzed in various adult rat tissues and in mammary glands of Wistar Furth rats at different developmental stages. As reported previously (18), p190-B cDNA is encoded by 6.4- and 4.4-kb transcripts. p190-B is expressed in several adult tissues including lung, liver, kidney, brain, and heart, and at much lower levels in ovary and uterus (data not shown).

Interestingly, p190-B was differentially expressed during mammary development. The highest level of expression was detected initially in the virgin mammary gland of 45-day-old rats and maintained in old virgin rats. p190-B mRNA levels then declined progressively during pregnancy through lactation (Fig. 5*A*). The relative levels of p190-B mRNA were compared with the level of K18 mRNA (Fig. 5*D*), a marker for ductal and alveolar epithelial cells, to correct for the changes on both epithelial cell content during mammary gland development and the dilution effect of abundant milk protein mRNAs during lactation. Using this correction, the relative expression of p190-B still decreased significantly during late pregnancy and lactation when compared with that of the 45-day-old virgin rats (Fig. 5*E*). The blot was also probed with β-casein to indicate the integrity of mRNA from pregnant and lactating glands (Fig. 5*C*). The relative decrease in expression of p190-B during pregnancy and lactation as compared with that in the virgin mammary gland may be attributed to the concomitant loss of TEBs with progressive differentiation. These findings, therefore, support the earlier observation of increased expression seen in the TEB fraction both by DD-PCR and *in situ* hybridization.

p190-B Is Overexpressed in Some Murine Mammary Tumors. On the basis of the observation that p190-B was expressed at higher levels in the less differentiated mammary gland (virgin mammary gland) and at stages representing increased proliferation (*i.e.*, 45-day virgin and early pregnancy), its expression was analyzed in a limited number of primary, rat NMU-induced tumors. Indeed, p190-B was highly expressed in 7 (35%) of 20 NMU-induced tumors analyzed. The expression level varied from 2-fold to several hundred-fold when compared with that of a 45-day- old rat virgin mammary gland, the time at which the animals received the carcinogen (Table 2 and Fig. 6; see *Lane 1* control *versus Lanes 3*, *4*, *9*, and *10*). p190-B expression in these samples was normalized using 28S RNA. Increased expression of p190-B mRNA was never observed in age-matched virgin animals [P = 0.000; *df*, 1; Fisher's exact test (two-tailed)], and was not changed as a function of aging. When the controls were more than 200 days old, none of the rats ever developed spontaneous tumors or displayed increased expression of p190-B in the normal mammary glands.

Interestingly, when *in situ* hybridization was used to identify the cell populations expressing p190-B mRNA, no detectable signal was observed in areas of the tumor that exhibited normal mammary epithelial histology (Fig. 7*A*; see *B* for representative histology of the region in *A*). In contrast, both the S and less-well-differentiated epithelium of the NMU-induced tumors expressed p190-B mRNA (Fig. 7*C*; see *D* for representative histology of the region in *C*). However, a second, more highly differentiated tumor, did not contain detectable p190-B transcripts (Fig. 7*E*; see *F* for representative histology of the region in *E*). In other tumors, p190-B expression was localized to regions that were also less well differentiated (data not shown). These studies suggest that

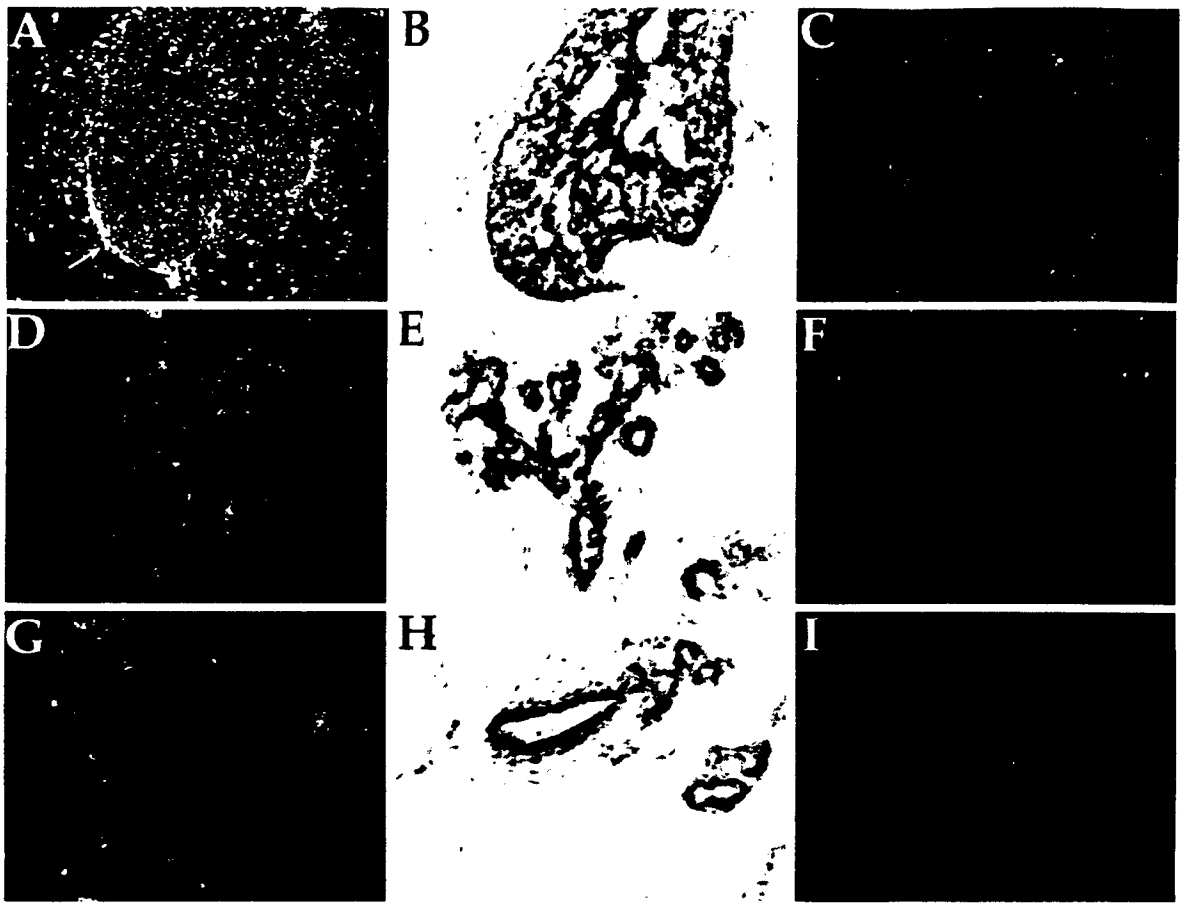

Fig. 4. In situ localization of *p190-B* gene expression in the virgin mammary gland. Dark field illuminations of ×200 fields showing hybridization to the *in vitro* transcribed ^{33}P-labeled p190-B transcripts. *A* (TEB), *D* (ABS), and *G* (Duct) show hybridization to the antisense transcripts. *B*, *E*, and *H* show the corresponding hematoxylin staining of the regions in *A*, *D*, and *G* at the same magnification. *C* (TEB), *F* (ABS), and *I* (Duct) show dark field illuminations of ×200 fields and hybridization to sense transcripts on a serial section.

the heterogeneous expression of p190-B that was observed in different NMU-induced tumors may be attributed to differences in epithelial cell types and/or epithelial-SI interactions in these tumors.

To determine whether p190-B expression was altered during cancer progression, its expression was also analyzed in a set of mouse TM tumors (20). TM tumors are grown by injecting TM cell lines into the mammary fat pad of syngeneic mice. p190-B expression was studied in these tumors because a complete spectrum of tumors ranging from hyperplastic nodules (HAN) to malignant tumors was available for study. Because the TM alveolar hyperplasias are morphologically similar to midpregnant mammary glands, p190-B expression in these hyperplasias and tumors was compared with that of a mouse at day 13 of pregnancy. p190-B expression in 7 (44%) of 16 tumors varied from 0.5- to 8-fold (Fig. 8 *top panel*; compare the control in *Lanes 1* to the tumor samples in *Lanes 4*, *5*, *6*, and *7*) when normalized with 28S RNA. In contrast, the level of expression ranged from 2- to 100-fold in NMU tumors.

These studies suggest that increased expression of p190-B mRNA may be associated with breast cancer. Although the functional significance of p190-B expression in hyperplasias and/or tumors remains to be investigated, this increase may reflect potentiation of the tumorigenic or invasive potential of these tumors. It is, however, important to note that the hyperplasias used in our study did not appear *de novo* but, instead, are maintained as transplants. It is possible that, under these circumstances, there was selection for p190-B expression *in vivo*. A more detailed analysis of p190-B expression in various other tumor types is in progress.

Contrary to the expected 6.4- and 4.4-kb transcripts, an additional 8.5-kb transcript was detected in all of the mouse tumor RNAs analyzed. To determine the origin of the third transcript, the blots were hybridized to both 5′ and 3′ specific probes from p190-B cDNA. The 3′ specific probe gave rise to the expected 6.4- and 4.4-kb transcripts. The 5′ probe, however, resulted in the detection of all of the three transcripts. The 5′ end of p190-B shares significant homology to the *p190-A* gene. The blot was, therefore, further hybridized to p190-A specific probe. This p190-A probe detected the 8.5-kb band (21). However, unlike p190-B, which displayed elevated expression in a few tumors as compared

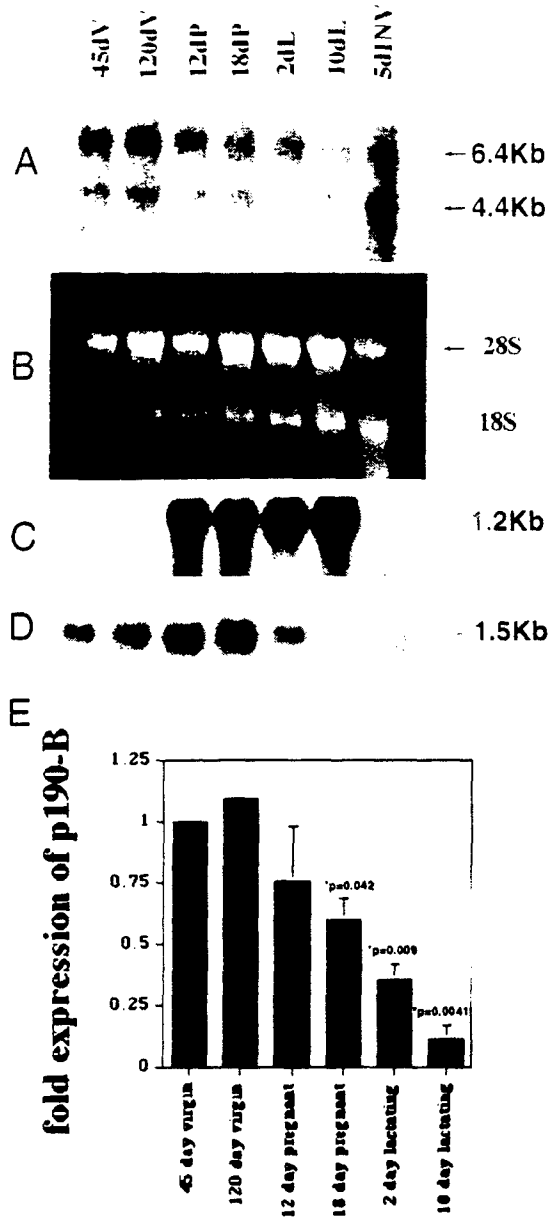

Fig. 5. Differential expression of p190-B during mammary development. Total cellular RNA (20 μg) from the fourth inguinal mammary gland was isolated from Wistar Furth rats at the following developmental stages: 45-day-old virgin (*45dV*), 120-day-old virgin (*120dV*), 12 days of pregnancy (*12dP*), 18 days of pregnancy (*18dP*), 2 days of lactation (*2dL*), 10 days of lactation (*10dL*), and 10 days of lactation followed by 5 days of involution, induced by forced removal of the pups from the mother (*5dINV*). *A*, total RNA hybridized to ^{32}P-labeled p190-B cDNA and exposed to films for 24–48 h. *B*, EtBr staining demonstrates equal loading of RNA. *C*, blot (as in *A*) stripped and rehybridized to β-casein cDNA. *D*, blot (as in *A*) stripped and rehybridized to K18 cDNA to normalize for epithelial content. The K18 signal was obtained from an 8–10-h exposure to the film as opposed to a 48-h exposure for the p190-B cDNA. *E*, phosphorimager quantitation of p190-B expression during mammary development. The blots were exposed to the phosphorimager for 24 h, and the results were quantitated using the software Imagequant (Molecular Dynamics). The ratio of p190-B:K18 expression is plotted as fold change over that of 45-day virgin expression in arbitrary volume units/μg RNA. *Error bars*, SE. Results are representative of three independent experiments. Because the RNA samples from *5dINV* showed some degradation, they were excluded from quantitative analysis.

Table 2 Summary of p190-B expression in NMU tumors and age-matched virgin mammary glands

Data were obtained from several independent Northern blot analyses. The percentage of tumor/glands with overexpression of p190-B are noted in parentheses.

	8- to 100-fold	2- to 4-fold	0- to 1-fold
Rat NMU tumors	7/20 (35)[a]	3/20 (15)[a]	10/20 (50)
Age-matched virgin	0/20 (0)	0/20 (0)	20/20 (100)

[a] Represents a significant difference from age-matched virgins. *P* is 0.000 (2-tailed Fisher's exact test).

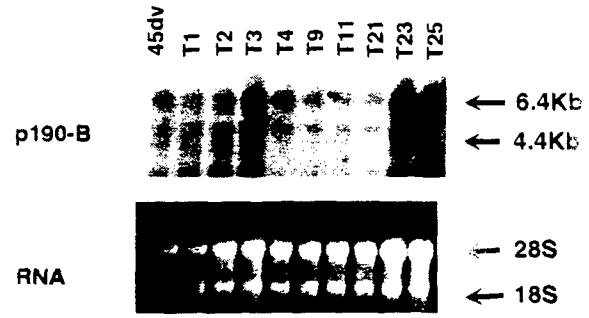

Fig. 6. Increased p190-B mRNA expression in some rodent mammary tumors. Total RNA (20 μg) from the indicated murine mammary tumors was hybridized to a ^{32}P-labeled p190-B cDNA and analyzed for p190-B expression using Northern blotting. *Top*, representative rat NMU- induced mammary tumors (*T1*, *T2*, *T3* and so forth) were analyzed for p190-B expression. *Left-most lane*, normal mammary gland RNA from a 45-day-old virgin rat (the time at which the animal received the carcinogen) was used as a control for analyzing overexpression in NMU tumors (loaded in *adjacent lanes*). *Bottom*, EtBr staining of the RNA gel.

with that observed in a 13-day pregnant mammary gland, p190-A expression was not detectable in the 13-day pregnant mammary gland. It was, however, detectable in all of the tumors analyzed (Fig. 8; compare the signal seen in bottom panel, *Lane 1*, with the signal seen in tumors run in *adjacent lanes*), which suggests that it also may be slightly up-regulated in all of the tumors analyzed in this study. However, because we did not see a direct correlation between the intensity of the 8.5-kb band in blots probed with the p190-B or the p190-A probes, it is difficult to conclude whether the third transcript in the mouse tumors is the result of cross-reactivity with p190-A transcript. It is possible that the third transcript represents an as yet unidentified isoform or a related gene transcript. This possibility has not been completely excluded, because the complete genomic structure of neither p190-B nor p190-A is known yet.

Overexpression of p190-B in MCF-10A Cells Results in Actin Cytoskeleton Disruption. Because overexpression of p190-B in TEBs and some less differentiated tumors suggested that it might facilitate invasion of TEBs into the fat pad during virgin mammary development and might also impart invasive potential to some rodent mammary tumors, we wanted to understand how p190-B might be implicated in signaling pathways that regulate ductal morphogenesis, cell transformation, and/or invasion. Although, a direct proof for its involvement in ductal morphogenesis can be obtained only from experiments carried out using p190-B knockout

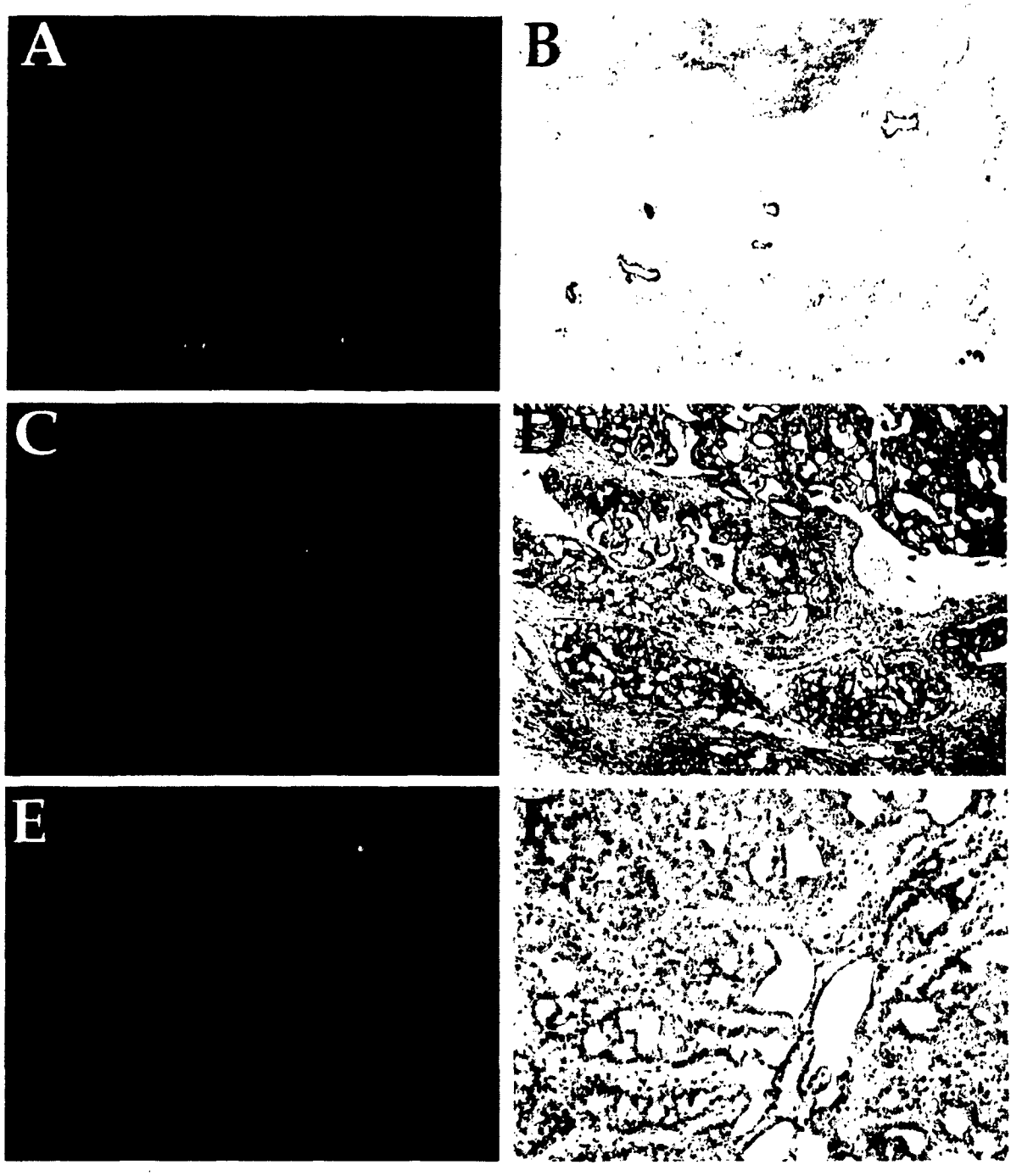

Fig. 7. Heterogeneous expression of p190-B in some rodent mammary tumors. *A*, *C*, and *E*, the dark field illumination of the tumor sections hybridized to the *in vitro* transcribed ^{33}P-antisense transcript for p190-B. The normal epithelium in *A* does not show hybridization to the probe. On the other hand, a strong hybridization signal is seen in both the epithelial and the S regions of the tumor in *C*. Because the tumor sections used for *in situ* analysis were stained with DAPI and visualized using fluorescence microscopy, H&E images from an adjacent section are included in *B*, *D*, and *F* as an illustration of the representative histology of the same tumor. All of the photomicrographs were taken at ×100. Data for sense controls are not shown.

mice mammary epithelium, as an initial step we, therefore, first tried to understand its role at the cellular level using transient transfection assays in an *in vitro* cell culture model.

A hallmark of all transformed epithelia is the loss of distinctive cell-to-cell contacts and the acquisition of migratory potential. p190-B, as a negative regulator of Rho proteins, may directly influence the adhesive capacity of a cell by affecting its actin stress fiber organization. We tested this hypothesis by analyzing the actin cytoskeletal architecture of p190-B-overexpressing cells. Accordingly, p190-B was tran-

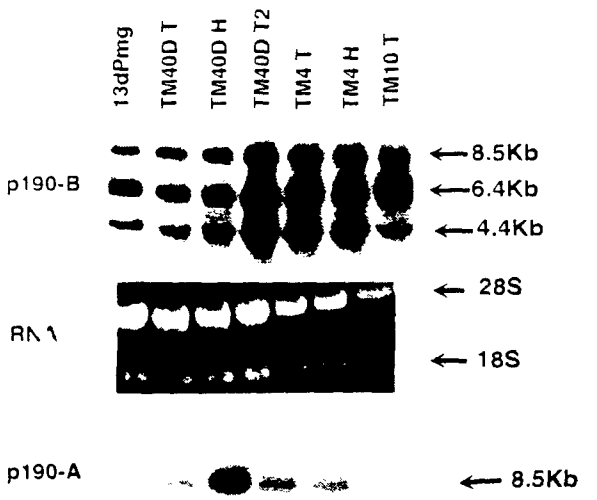

Fig. 8. p190-B mRNA expression in some murine mammary tumors. *Top*, representative mouse TM mammary tumors analyzed for p190-B expression. *Left lane*, total RNA from normal mammary gland of a 13-day pregnant C57BL/6 mice was used as a control for comparing the levels as seen in tumor RNA samples designated TM4, TM10, or TM40D. T and H extensions have been used to indicate a tumor or a hyperplasia. *Middle*, EtBr staining of the gel. *Bottom*, The blot was stripped and hybridized to p190-A cDNA to confirm the origin of the third transcript seen in mouse tumor RNA panel.

siently transfected into MCF-10A human mammary epithelial cells using an efficient adenovirus-mediated transfection protocol (29). The MCF-10A cells have been characterized as spontaneously immortalized, nontumorigenic, human breast epithelial cells with a near diploid karyotype (23), and they possess many of the markers characteristic of a normal mammary epithelial cell. The function of p190-B was assessed by the simultaneous analysis of actin stress fiber organization in p190-B-expressing cells grown on coverslips using double immunofluorescence staining (see "Materials and Methods"). The FITC-phalloidin staining pattern in the p190-B expressing cells was circumferential as opposed to the fine overall network of actin stress fibers observed in mock-transfected cells (Fig. 9; compare *A* and *C* with *B* and *D*). p190-B expression in these transfected cells appeared to be punctate in the cytoplasm and was not localized at focal adhesions, as might be expected if these cells had been grown on an ECM. However, double immunofluorescence staining was used only to identify transfected cells and not to study subcellular localization of p190-B under different culture conditions. In addition—despite using appropriate antibody dilutions to minimize background staining problems—weak nuclear staining, which may be the result of nonspecific cross-reactivity of the HA monoclonal antibody, was seen in some mock-transfected and 190-B-transfected cells.

Eighty-four % of p190-B-transfected cells exhibited a significantly reduced actin stress fiber network (Fig. 10*A*, ▨), as compared with only 9% of the mock-transfected cells (Fig. 10*A*, ■). In addition, the majority of p190-B-transfected cells exhibited a tendency to detach from the MCF-10A cell clusters, and to remain as single, isolated cells (60%) or in pairs detached from the cell monolayer (Fig. 10*B*; compare ▨ with ■). When we further compared the tendency of both transfected and mock-transfected cells to remain attached to the cell monolayer, approximately 30% transfected cells (Fig. 10C, ▨), as compared with 80% mock transfected cells (Fig. 10C, ■), were found attached to the monolayer. These studies suggest that p190-B over-expression results in a disruption of the actin cytoskeleton, which may, in turn, make the cells less adherent, an important step in cell migration and invasion.

Discussion

Both epidemiological studies and carcinogenesis experiments in rats indicate that hormonal changes during pregnancy exert a protective effect on breast cancer. Because rat and human mammary glands have similar developmental patterns and structural features, the rat has been used as a model system to identify the mechanism by which these hormones confer resistance (24). Postnatal mammary development in rats commences during the 1st week after parturition. The primary duct branches into three to five secondary ducts. The distinctive club-shaped structures at the distal ends of the mammary ducts are the TEBs (25). During adolescent mammary development the systemic hormones act on TEBs to stimulate proliferation and rapid ductal elongation into the mammary fat pad (8). Carcinogenesis studies in rats have revealed that TEBs are also the major site for carcinogen-induced DNA damage (7). Experiments were, therefore, initiated to isolate genes that were differentially expressed between TEBs, TDs, and S using a combination of DD-PCR and Reverse Northern techniques. Fourteen DD-PCR products, found primarily in the TEB Lanes of DD-PCR gels, were isolated, subcloned and sequenced, and compared with GenBank entries.

Although DD-PCR was the most suitable technique available at the time, two serious drawbacks were encountered: the generation of short 3′ clones and the high incidence of false positives. The latter problem could be circumvented to some extent by confirming the DD-PCR results by Reverse Northern analysis. However, some of the clones did not provide a significant signal over background and were still below the level of detection by Reverse Northern using the phosphorimager for quantitation. In addition, because the TEBs and the M and S fractions were manually dissected from trypan blue-injected mammary glands of 10 different animals, the pooled fractions of RNA isolated were contaminated with tissue from the S. The availability of more recent techniques like laser-capture microdissection should eliminate these problems in future.

Despite these limitations, p190-B was found to be preferentially expressed in the TEBs. p190-B is a Rho-Gap member that is recruited to the sites of integrin clustering (18). It encodes a protein with an NH_2-terminal GTPase domain and a COOH-terminal Rho-Gap domain that stimulate the intrinsic GTPase activity of Rho, Rac, and cdc-42, thereby functioning as a negative regulator of their signal-transducing activity. p190-B shares some features in common with several members of the Ras, Rab, Ral, and Rho family of GTPases, but it is most closely related

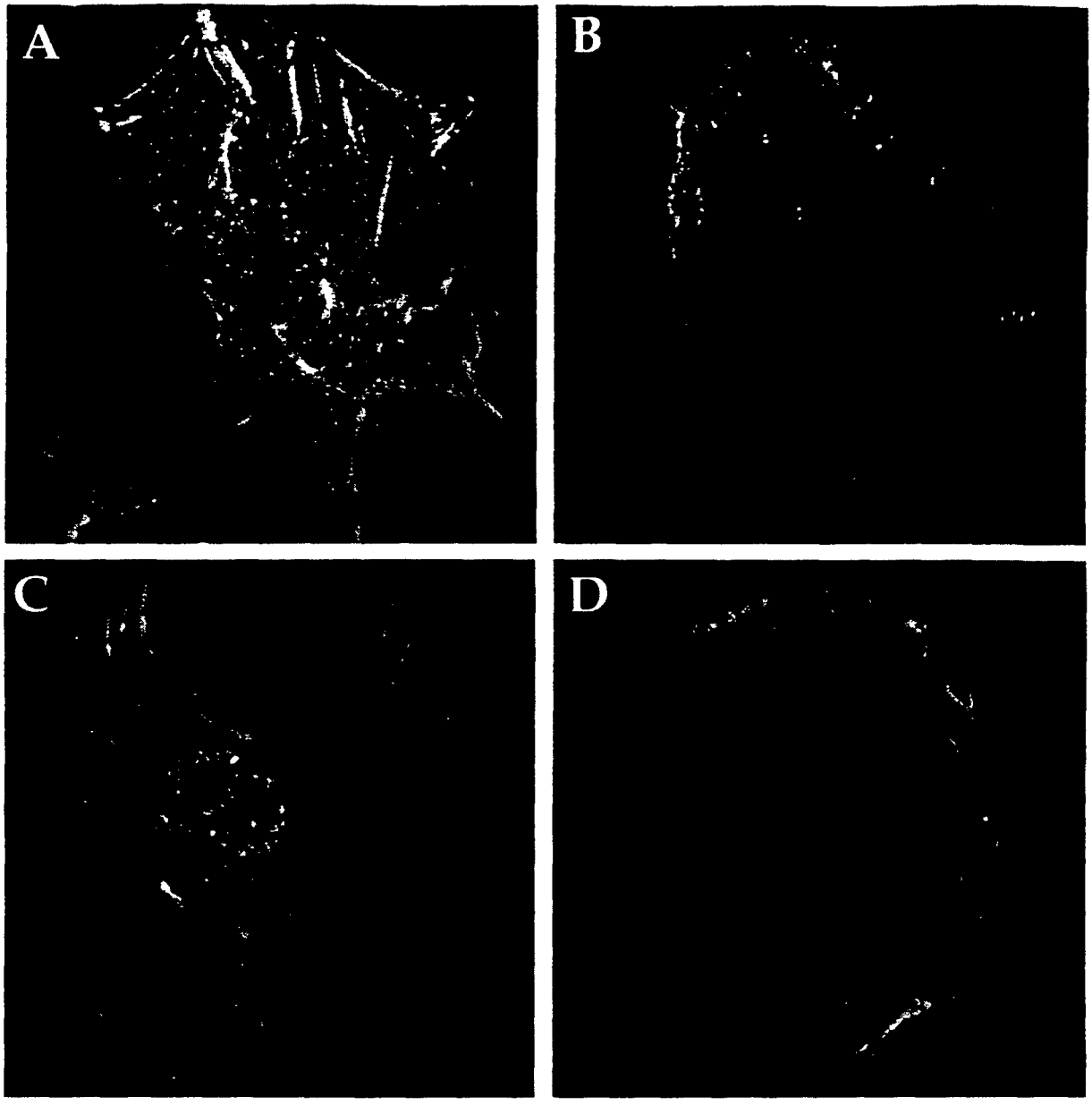

Fig. 9. p190-B-induced actin cytoskeletal reorganization in MCF-10A cells. MCF-10A cells were transiently transfected either with the vector alone or with a p190-B expression construct and were grown on coverslips, fixed, and simultaneously stained with anti-HA antibody and FITC-phalloidin, as described in "Materials and Methods." *A* and *C*, vector-transfected control cells. *B* and *D*, cells transfected with a HA-tagged p190-B construct. The p190-B transfected cells have a markedly reduced actin stress fiber network and exhibit circumferential staining for actin. All of the photomicrographs were taken on a DeltaVision deconvolution microscope using the ×63 lens.

to p190-A, sharing 51% amino acid identity (see review 26). The sequences of both p190-A and -B are conserved among mouse, rats, and humans. In the present studies, differential expression of p190-B in TEBs of the rat virgin mammary gland and an increased expression in some less-well-differentiated murine mammary tumors were observed. Although the functional significance of increased p190-B expression in tumors remains to be investigated, overexpression of p190-B in "normal" human mammary epithelial cells resulted in the disruption of the actin cytoskeleton, which suggests, therefore, that it may facilitate cell migration and invasion. The direct involvement of Rho-Gaps in invadopodia formation in LOX melanoma cells has also been reported (27). The Rho family of proteins have been implicated in the regulation of multiple signal transduction processes and are key components for the transforming action of diverse oncoproteins (reviewed in Ref. 28). They are also induced in response to receptor tyrosine kinase activation in human mammary epithelial cells, breast cancer tissues, and cell lines (29).

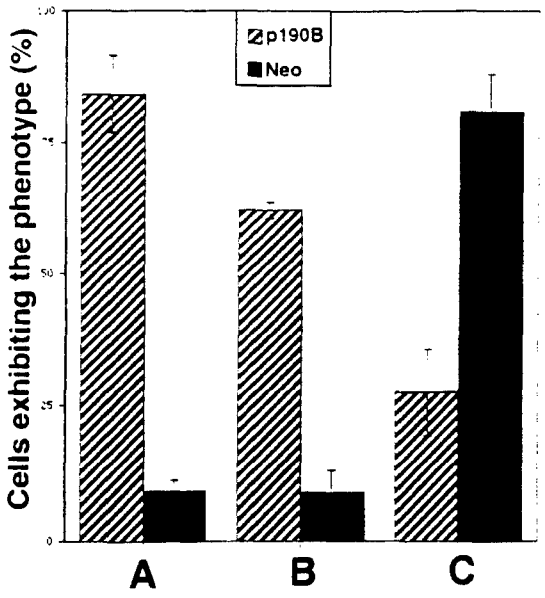

Fig. 10. A total of 100 cells each of transfected (▨) and vector-transfected cells (■) were scored for the loss of actin fibrils (*A*), the presence of single isolated cells (*B*), and whether the cells were attached to the monolayer (*C*). The data were normalized for transfection efficiency. *Error bars*, SE from three separate experiments.

The *p190-B* gene has been localized recently to mouse chromosome 12 and has been mapped to the conserved region of human chromosome 14; the closest linkage was to hsp70, which is located on 14q22–24 (30). This region has been shown to be amplified in a restricted group of human breast cancers (31), and to be deleted in ductal carcinoma *in situ* of the breast (32) by comparative genomic hybridization, thereby supporting the suggestion that the inappropriate regulation of this locus may be a factor in the etiology of breast cancer. Both the RNA expression profile during mammary development and the tissue distribution of p190-B suggest that p190-B may be required for ductal morphogenesis during virgin mammary gland development and that its aberrant expression may occur in aggressive tumors. The hypothesis that p190-B facilitates cell invasion by orchestrating the ECM-mediated integrin signals through Rho proteins, remains to be tested using stably transfected MCF-10A cells, with which it may be possible to study gain-of-function and loss-of-function mutants, and *in vivo* by generating a mammary gland-specific knockout of this gene.

Materials and Methods

Animals. Wistar Furth rats with an inbred genetic background were obtained from Harlan Sprague Dawley Inc. All of the animals were maintained and killed according to IACUC-approved guidelines.

Tumor Tissues. Dr. Daniel Medina (Baylor College of Medicine, Houston, TX) provided the NMU-induced rat and mouse TM tumors.

Probes. A full-length p190-B cDNA construct was a generous gift of Dr. Peter Burbelo (Laboratory of Developmental Biology, National Institute of Dental Research), Dr. Jeffrey Settleman, Laboratory of Signal Transduction (Massachusetts General Hospital Cancer Center, Charlestown, MA) kindly provided the p190-A cDNA.

Antibodies. Mouse monoclonal antibody (clone 12CA5) for HA epitope tag was purchased from Boehringer Mannheim. FITC- phalloidin (Sigma) was a gift from Dr. Bill Brinkley.

Adenovirus. Adenovirus stocks were purchased from Dr. Nancy Weigel's laboratory at Baylor College of Medicine.

Mammary Gland Tissue Isolation by Dye Visualization. TEBs and M and S tissue were isolated from the fourth inguinal mammary glands of nulliparous 42–45-day-old rats in the following manner. After making a midline incision, the skin was separated from the peritoneum, and the mammary gland was exposed. To visualize the mammary ductal structure, the top portion of the fourth nipple was removed, and the visualization dye (0.5% trypan blue w/v in PBS) was injected using a 26-G needle. After complete infiltration of the dye throughout the ductal tree, the three fractions were easily identified and surgically isolated (see Fig. 1). The tissue sections were snap-frozen in liquid nitrogen and transferred to −80°C for storage until used for isolation of RNA.

Isolation and Identification of DD-PCR Clones. RT-PCR and PCR reactions were performed with the materials provided and the protocols recommended for use of the RNAimage kit (GenHunter Corp. Brooklyn, MA). Total RNA was prepared from each tissue region using 4-M guanidium isothiocyanate and CsCl buoyant-density centrifugation (33). For each sample, two sets of three RT reactions were prepared as per a previously described procedure (16). The RT samples were then amplified by low-stringency PCR in the presence of 20 pmol of α-^{35}S-labeled dNTP (1200 Ci/mmol), the T-specific primer used in the RT reaction in combination with various random 11mers supplied with the kit, and 2.5 U of Ampli Taq polymerase (Perkin-Elmer Applied Biosystems).

To identify the differentially expressed genes, DD-PCR products of the three starting RNA populations (TEB, M, and S) were run on a denaturing polyacrylamide gel, transferred to 3-mm Whatman paper, dried, and exposed to X-ray film (Eastman Kodak). To confirm the reproducibility of the banding pattern, each representative RT reaction was performed from two independent pools of RNA for each of the three regions (TEB, M, and S regions). Bands that were more intense in the TEB fraction were excised from the gel and reamplified. The PCR reaction was similar to the previous reaction except with 20 μM dNTP and no labeled nucleotide. The PCR products so generated were initially cloned into PCR-TRAP vector and then subcloned into *Hin*dIII site of pBluescript II (Stratagene).

Sequencing and Identification of DD-PCR Products. The cloned DD-PCR products, termed EDD clones were sequenced by standard dideoxy chain termination methods. Both of the strands were sequenced using T7 and T3 primers. BLAST search combined with masker was used to compare the clone sequences with GenBank.

Preparation and Analysis of Total RNA. The fourth inguinal mammary glands from virgin, pregnant, and lactating rats were dissected under anesthesia using standard surgical procedures. Tissue was snap-frozen in liquid nitrogen and stored at −80°C. Total cellular RNA was prepared using 4 M guanidium isothiocyanate and CsCl buoyant-density centrifugation (33). RNA was fractionated on a 1.2% formaldehyde agarose gel and transferred to Hybond N+ (Amersham) membrane with 10× SSC. Hybridization was performed in Hybaid oven at 65°C using procedures recommended by Amersham. The filters were quantitated for 16–48 h using the PhosphorImager (Molecular Dynamics). The data were normalized to the 28S rRNA signal.

Screening of High-Density Blots by Reverse Northern. First strand ^{32}P-cDNA was synthesized from 5–6 μg of total RNA from EB, M, and S fractions of the virgin mammary gland using superscript II RT (Life Technologies, Inc.) in the presence of 1 μg of oligo(dT)$_{12-18}$mer primers as per manufacturer's instructions. The cDNA was hydrolyzed by NaOH treatment and neutralized with HCl treatment. The labeled cDNA was then purified through a sephadex G50 column. The efficiency of the reaction was monitored by determining the total radioactivity incorporated before and after purification of the probe.

A total of eight DD-PCR clones and three control plasmids (K18, RPL19, and GAPDH) were subjected to PCR amplification. After amplification, a fixed amount of each of the PCR products was loaded onto high-density gels in triplicate (Centipede gel electrophoresis chambers; Owl Scientific, Woburn, MA). PCR products were alkali-denatured in the gel and blotted onto nylon membranes. The filters were hybridized with equivalent amounts of ^{32}P-labeled single-stranded cDNA (specific activity, 1 × 10^9 cpm/μg) from TEB, M, and S regions of the virgin mammary gland. The filters were washed under stringent conditions as per the Church and Gilbert method (34) and quantitated using the phospho-

mager. In addition, the filters were exposed to high-resolution Kodak Biomax MR films for up to 24 h at −80° C.

***In Situ* Hybridization.** Riboprobes were labeled with [^{33}P]UTP (2500 Ci/mmol; Amersham), using the appropriate T3 or T7 transcription systems from Stratagene. To generate the riboprobe templates, the cDNA was linearized with a restriction enzyme so as to make an antisense transcript that originates from the more divergent 3′ end of the cDNA, thus making it more specific for p190-B. ^{33}P-riboprobes were used because, unlike ^{35}S, ^{33}P gives less background, and very high specific-activity probes can be generated for the detection of rare transcripts. The ^{33}P-riboprobe was purified on a sephadex G50 column and counted in a scintillation counter.

Pretreatment of Slides and Hybridization. The fourth inguinal mammary glands from virgin Wistar Furth rats were excised and immediately fixed for 3 h in ice-cold 4% paraformaldehyde in PBS, dehydrated in a graded series of ethanols to xylene, and embedded in paraffin wax. Sections of 4–5 μm were mounted on ProbeOn Plus slides (Fisher Biotech). Sections were baked overnight at 37°C, dewaxed through xylene, and rehydrated through a graded series of ethanols to PBS. After digestion with proteinase K (20 μg/ml; Sigma) at 50°C for 5 min, the sections were refixed in 4% paraformaldehyde/PBS for 5 min. The sections were then acetylated in 100 mM triethanolamine and 25 mM acetic anhydride and was dehydrated through ethanols. Sections were prehybridized in 2× SSC, 50% formamide, 10% dextran sulfate, 1% SDS, and 500 ng/ml denatured herring sperm DNA at 37°C in a sealed humidified chamber. ^{33}P-labeled riboprobe (1×10^5 cpm/μl) was diluted into 25 μl of hybridization solution, which was then added to the solution already covering the section. The sections were hybridized overnight at 42°C in a sealed humidified chamber. The sections were subsequently washed in 2× SSC at 55°C with the last wash in 0.1× SSC at 55°C.

Detection of the Radioactive Signal. The sections were dehydrated in a graded series of ethanol/water containing 0.3 M sodium acetate. The sections were air-dried and coated with NTB2 nuclear emulsion (Eastman Kodak Co, NY) and exposed in light-proof slide boxes for 48–72 h. After development (as per Kodak instructions), the sections were stained with either hematoxylin or DAPI and visualized using dark-field microscopy in combination with bright-field or fluorescence microscopy.

Construction of p190-B Expression Vector. The expression plasmid was generated from an E3 plasmid[4] provided by Dr. Peter Burbelo (Laboratory of Developmental Biology, NIDR), which contains the complete coding sequence of p190-B with flanking 5′ and 3′ untranslated sequences. A 1.2-kb *Kpn*I-*Eco*RV fragment from the 5′ end was tagged at the NH_2 terminus with an HA sequence (nine amino acids; YPYDVPDYA; Ref. 35) by PCR using the forward primer: 5′-CCGGTACCATGGGGTACCCATACGACGTCCCAGACTACGCTGCAAAAAACAAAGAGCCTCGTCCCCCATCC (71mer), and the reverse primer: 5′-CTCGTGAAATCTTCGACTTTTTCAGATAGTCTTGGTACATGTCGTAGACTATAGGCTCTTCTCCTC (66mer), with linearized E3 plasmid as the template. PCR was carried out as follows: denaturation at 95°C for 5 min, followed by 25 cycles of denaturation for 30 s at 95°C, annealing at 65°C for 3′ extension for 3 min at 72°C, after 10 min extension at 72°C. This fragment was engineered to have a *Kpn*I site at the 5′ end and a consensus Kozak sequence before the starting ATG. The generated fragment was cloned into *Kpn*I-*Eco*RV site of PCR3.1 vector (Invitrogen). This vector was further cut with *Eco*RV and *Not*I to accommodate a 3′ *Eco*RV-*Not*I fragment from the E3 plasmid. A *Kpn*I-*Not*I fragment from this second-generation construct represents the complete coding region of p190-B and about 180bp of 3′ untranslated region.

Cell Culture and Transfection. Human breast epithelial cells (MCF-10A) were obtained from Barbara Ann Karmanos Cancer Institute (passage 149) and cultured in DMEM:F12 Media (1:1) supplemented with 5% serum, insulin (10 μg/ml), epidermal growth factor (20ng/ml), cholera toxin (100ng/ml), hydrocortisone (0.5 μg/ml), penicillin 100 units/ml, streptomycin (100 μg/ml), and fungizone (0.5 μg/ml). Cells were split 1:3 to 1:4 and passaged every 3–4 days. MCF-10A cells (2×10^5) were seeded onto coverslips 24 h before transient transfection and transfected with either 2 μg of p190-B expression plasmid or the control vector using adenovirus-DNA-lysine cocktail in serum-free media (22). To normalize for transfection efficiency, 400 ng of cytomegalovirus β-galactosidase was cotransfected as a tracer. Twelve h after transfection, the cells were switched to complete media for another 24–36 h. The cells were fixed and stained for simultaneous detection of p190-B and the actin cytoskeleton, as described previously (36). The anti-HA antibody was used at a dilution of 1:500, whereas FITC-phalloidin was used at a dilution of 1:1000. Goat antimouse IgG (Santa Cruz Biotechnology) conjugated with Texas Red was used as the secondary antibody against HA-antibody. The cells were analyzed by indirect immunofluorescence, and images were collected at 5-μm steps using a DeltaVision deconvolution microscope from Applied Precision, Inc. (Issaquah, WA). Thirty of such 5-μm images were rendered to make a projection using the softWoRx imaging workstation (also from Applied Precision, Inc.).

[4] P. Burbelo, unpublished data.

Acknowledgments

We thank Drs. D. Medina and N. Greenberg for their critical evaluation of the manuscript; Dr. Peter Burbelo, Laboratory of Developmental Biology, NIDR, for providing the p190-B cDNA; and Dr. Jeffrey Settleman (Laboratory of Signal Transduction, ~~MGH~~ Cancer Center) for providing the p190-A cDNA. We thank Dr. D. Medina (Baylor University, Houston, TX) for also providing the mouse and rat tumor samples. Special thanks to Frank Herbert from the Cell Biology Microscopy Core and Dr. Elena B. Kabotyanski for helping with the deconvolution microscopy.

Massachusetts General Hospital, Charlestown, MA 02129, US

References

1. MacMahon, B., Cole, P., Lin, T. M., Lowe, C. R., Mirra, A. P., Ravnihar, B., Salber, E. J., Valaoras, V. G., and Yuasa, S. Age at first birth and breast cancer risk. Bull. WHO, *43:* 209–221, 1970.

2. Sinha, D. K., Pazik, J. E., and Dao, T. L. Prevention of mammary carcinogenesis in rats by pregnancy: effect of full-term and interrupted pregnancy. Br. J. Cancer, *57:* 390–394, 1988.

3. Yang, J., Yoshizawa, K., Nandi, S., and Tsubura, A. Protective effects of pregnancy and lactation against *N*-methyl-*N*- nitrosourea-induced mammary carcinomas in female Lewis rats. Carcinogenesis (Lond.), *20:* 623–628, 1999.

4. Thordarson, G., Jin, E., Guzman, R. C., Swanson, S. M., Nandi, S., and Talamantes, F. Refractoriness to mammary tumorigenesis in parous rats: is it caused by persistent changes in the hormonal environment or permanent biochemical alterations in the mammary epithelia? Carcinogenesis (Lond.), *16:* 2847–2853, 1995.

5. Grubbs, C. J., Farnell, D. R., Hill, D. L., and McDonough, K. C. Chemoprevention of *N*-nitroso-*N*-methylurea-induced mammary cancers by pretreatment with 17β-estradiol and progesterone. J. Natl. Cancer Inst., *74:* 927–931, 1985.

6. Medina, D., and Smith, G. Chemical carcinogen-induced tumorigenesis in parous, involuted mouse mammary glands. J. Natl. Cancer Inst., ~~1999~~ 91: 967–969, 1999

7. Russo, J., and Russo, I. H. Biological and molecular bases of mammary carcinogenesis. Lab, Investig., *57:* 112–137, 1987.

8. Topper, Y. J., and Freeman, C. S. Multiple hormone interactions in the developmental biology of the mammary gland. Physiol. Rev., *60:* 1049–106, 1980.

9. Sivaraman, L., Stephens, L. C., Markaverich, B. M., Clark, S. Krnacik, J. A., Conneely, O. M., O'Malley, B. W., and Medina, D. Hormone-induced refractoriness to mammary carcinogenesis in Wistar- Furth rats. Carcinogenesis (Lond.), *19:* 1573–1581, 1998.

10. Guzman, R. C., Yang, J., Rajkumar, L., Thordarson, G., Chen, X., and Nandi, S. Hormonal prevention of breast cancer: mimicking the protective effect of pregnancy. Proc. Natl. Acad. Sci. USA, *96:* 2520–2525, 1999.

11. Humphreys, R. C., Lydon, J., O'Malley, B. W., and Rosen, J. M. Mammary gland development is mediated by both stromal and epithelial progesterone receptors. Mol. Endocrinol., *11:* 801–811, 1997.

12. von Stein, O. D., Thies, W. G., and Hofmann, M. A high throughput screening for rarely transcribed differentially expressed genes. Nucleic Acids Res., *25:* 2598–2602, 1997.

13. Schena, M. Genome analysis with gene expression microarrays. BioEssays, *18:* 427–431, 1996.

14. Lisitsyn, N., and Wigler, M. Cloning the differences between two complex genomes. Science (Washington DC), *259:* 946–951, 1993.

15. Carulli, J. P., Artinger, M., Swain, P. M., Root, C. D., Chee, L., Tulig, C., Guenn, J., Osborne, M., Stein, G., Lian, J., and Lomedico, P. T. High throughput analysis of differential gene expression. J. Cell. Biochem. Suppl., *30–31:* 286–296, 1998.

16. Liang, P., and Pardee, A. B. Differential display of eukaryotic messenger RNA by means of the polymerase chain reaction. Science (Washington DC), *257:* 967–971, 1992.

17. Altschul, S. F., Madden, T. L., Schaffer, A. A., Zhang, J., Zhang, Z., Miller, W., and Lipman, D. J. Gapped BLAST and PSI-BLAST: a new generation of protein database search programs. Nucleic Acids Res., *25:* 3389–3402, 1997.

18. Burbelo, P. D., Miyamoto, S., Utani, V. Brill, S., Yamada, K. M., Hall, A., and Yamada, Y. p190-B, a new member of the Rho GAP family, and Rho are induced to cluster after integrin cross-linking. J. Biol. Chem., *270:* 30919–30926, 1995.

19. Keely, P., Parise, L., and Juliano, R. Integrins and GTPases in tumour cell growth, motility and invasion. Trends Cell Biol., *8:* 101–106, 1998.

20. Medina, D., Kittrell, F. S., Liu, Y. J., and Schwartz, M. Morphological and functional properties of TM preneoplastic mammary outgrowths. Cancer Res., *53:* 663–667, 1993.

21. Settleman, J., Narasimhan, V., Foster, L. C., and Weinberg, R. A. Molecular cloning of cDNAs encoding the GAP-associated protein p190: implications for a signaling pathway from ras to the nucleus. Cell, *69:* 539–549, 1992.

22. Allgood, V. E., Zhang, Y., O'Malley, B. W., and Weigel, N. L. Analysis of chicken progesterone receptor function and phosphorylation using an adenovirus-mediated procedure for high-efficiency DNA transfer. Biochemistry, *36:* 224–232, 1997.

23. Soule, H. D., Maloney, T. M., Wolman, S. R., Peterson, W. D., Jr., Brenz, R., McGrath, C. M., Russo, J., Pauley, R. J., Jones, R. F., and Brooks, S. C. Isolation and characterization of a spontaneously immortalized human breast epithelial cell line, MCF-10. Cancer Res., *50:* 6075–6086, 1990.

24. Russo, J., and Russo, I. H. Experimentally induced mammary tumors in rats. Breast Cancer Res. Treat., *39:* 7–20, 1996.

25. Russo, J., Tay, L. K., and Russo, I. H. Differentiation of the mammary gland and susceptibility to carcinogenesis. Breast Cancer Res. Treat., *2:* 5–73, 1982.

26. Scheffzek, K., Ahmadian, M. R., and Wittinghofer, A. GTPase-activating proteins: helping hands to complement an active site. Trends Biochem. Sci., *23:* 257–262, 1998.

27. Nakahara, H., Mueller, S. C., Nomizu, M., Yamada, Y., Yeh, Y., and Chen, W. T. Activation of beta1 integrin signaling stimulates tyrosine phosphorylation of p190RhoGAP and membrane-protrusive activities at invadopodia. J. Biol. Chem., *273:* 9–12, 1998.

28. Zohn, I. M., Campbell, S. L., Khosravi-Far, R., Rossman, K. L., and Der, C. J. Rho family proteins and Ras transformation: the RHOad less traveled gets congested. Oncogene, *17:* 1415–1438, 1998.

29. de Cremoux, P., Gauville, C., Closson, V., Linares, G., Calvo, F., Tavitian, A., and Olofsson, B. EGF modulation of the ras-related rhoB gene expression in human breast- cancer cell lines. Int. J. Cancer, *59:* 408–415, 1994.

30. Burbelo, P. D., Finegold, A. A., Kozak, C. A., Yamada, Y., and Takami, H. Cloning, genomic organization and chromosomal assignment of the mouse *p190-B* gene. Biochim. Biophys. Acta, *1443:* 203–210, 1998.

31. Courjal, F., and Theillet, C. Comparative genomic hybridization analysis of breast tumors with predetermined profiles of DNA amplification. Cancer Res., *57:* 4368–4377, 1997.

32. James, L. A., Mitchell, E. L., Menasce, L., and Varley, J. M. Comparative genomic hybridisation of ductal carcinoma *in situ* of the breast: identification of regions of DNA amplification and deletion in common with invasive breast carcinoma. Oncogene, *14:* 1059–1065, 1997.

33. Chirgwin, J. M., Przybyla, A. E., MacDonald, R. J., and Rutter, W. J. Isolation of biologically active ribonucleic acid from sources enriched in ribonuclease. Biochemistry, *18:* 5294–5299, 1979.

34. Church, G. M., and Gilbert, W. Genomic sequencing. Proc. Natl. Acad. Sci. USA, *81:* 1991–1995, 1984.

35. Wilson, I. A., Niman, H. L., Houghten, R. A., Cherenson, A. R., Connolly, M. L., and Lerner, R. A. The structure of an antigenic determinant in a protein. Cell, *37:* 767–778, 1984.

36. Kazansky, A. V., Kabotyanski, E. B., Wyszomierski, S. L., Mancini, M. A., and Rosen, J. M. Differential effects of prolactin and src/abl kinases on the nuclear translocation of STAT5B and STAT5A. J. Biol. Chem., *274:* 22484–22492, 1999.